# Requiem on the positive effects of commercial adaptive cruise control on motorway traffic and recommendations for future automated driving systems

Biagio Ciuffo [a], Konstantinos Mattas [a], Michail Makridis [a,b], Giovanni Albano [f],
Aikaterini Anesiadou [g], Yinglong He [c], Szilárd Josvai [d], Dimitris Komnos [h],
Marton Pataki [d,e], Sandor Vass [e], Zsolt Szalay [d,e,*]

[a] European Commission – Joint Research Centre, Ispra, VA, Italy
[b] ETH Zürich, Institute for Transport Planning and Systems (IVT), Zürich, CH, Switzerland
[c] University of Birmingham, Edgbaston, Birmingham B15 2TT, UK
[d] ZalaZONE - Automotive Proving Ground Zala Ltd., Zalaegerszeg, Hungary
[e] Department of Automotive Technologies, Budapest University of Technology and Economics, Budapest, Hungary
[f] Seidor Italia Srl, Milan, Italy
[g] Independent Consultant
[h] Fincons Group, Vimercate, Italy

## ARTICLE INFO

## ABSTRACT

Connected and automated vehicles (CAVs) promise to significantly improve road traffic. To a certain extent, this situation is similar to the expectations at the end of the last century about the positive effects that the introduction of Adaptive Cruise Control (ACC) systems would have had on motorway traffic. The parallelism is interesting because ACC equipped vehicles represent the first level of vehicle automation and are now widely available on the market. In this light, studying ACC impacts can help to anticipate potential problems related to its widespread application and to avoid that AVs and CAVs will lead to the same problems.

Only a few test-campaigns had been carried out studying the ACC impacts under real-world driving conditions in quantitative terms. To bridge this gap, the Joint Research Centre of the European Commission has organized a number of experimental campaigns involving several ACC-equipped vehicles to study different implications of their widespread. In this context, the present paper summarizes the outcomes of a test campaign involving 10 commercially available ACC-equipped vehicles. The test campaign has been executed in two different test-tracks of the ZalaZONE proving ground, in Hungary. The tests have been carried out at low-speeds (30–60 km/h) and have involved platoons of vehicles of different brands and different powertrains, which were tested in a variety of vehicle orders and with different settings of their ACC systems. Test results have been used to derive information about the properties of the different ACC systems, to study their string stability, to study the effect of ACC systems on traffic flow, and to draw inference about the possible implications on energy consumption and traffic safety.

Results confirm the previous findings in terms of string instability of the ACC and highlight that in the present form, ACC systems will possibly lead to higher energy consumption and introduce new safety risks when their penetration in the fleet increases. However, they also highlight that

---

* Corresponding author.
  *E-mail address:* zsolt.szalay@auto.bme.hu (Z. Szalay).

the materialization of the above findings for AVs depends on the operational logic that manufacturers will adopt during the implementation phase. Therefore, results suggest that functional requirements to guarantee string stability and in general to not disrupt the normal flow of traffic should be introduced both for ACC and for any automated system that will be placed on the market in the future.

## 1. Introduction

Vehicle automation and connectivity are expected to radically transform road transportation in the years to come (Alonso Raposo and (Ed.), 2019). By accurately sensing the environment and continuously communicating with the surrounding vehicles and the infrastructure, connected and automated vehicles (CAVs) will have the possibility to promptly adapt their driving operations to the surrounding conditions. Many authors have already started to study the potential benefits in increasing road capacity, avoiding traffic string instability, preventing shockwave formation, reducing fuel consumption and emissions as a result of smoother operations, and so on, for different CAVs penetration levels. Unfortunately, most of these studies are based on hypothetical assumptions on the logic governing future vehicles and on the performances of their sensing and communication systems. Alonso Raposo, 2019 have already warned that these benefits may take significantly more time than expected to materialize and will very much depend on the functional requirements vehicle manufacturers will have to fulfill in developing them. As the effect on traffic is usually not among the dimensions considered in vehicle regulations, the risk that CAVs may not improve current traffic dynamics (or even worsen them) is significant.

To understand the likelihood that this will happen, the authors of the present paper have studied the effect on traffic flow dynamics and some traffic externalities of one of the precursors of future automated driving systems, the Adaptive Cruise Control (ACC). ACC is nowadays one of the most common Advanced Driving Assistance Systems (ADAS) available in market vehicles. As with CAVs today, when they started to appear more than twenty years ago, many authors had indicated the potential benefits ACC could have brought to motorway traffic. From this point of view, the lessons that we can learn from ACC can be very useful to understand what may happen in the future with CAVs. It is worth mentioning here that in developing their ACC logics vehicle manufacturers had very limited requirements to fulfill. Since it is considered a comfort feature and the driver is always deemed responsible for supervising its operations, there are no legislative requirements for its market introduction. On the contrary, since CAVs will bear responsibility for driving operations, ad hoc requirements and validation methods are currently being developed to assess their capability to safely drive in real traffic conditions (UNECE, 2020a). If such requirements will not take into account the effect on traffic flow, CAVs' positive effect on traffic and related externalities will be even less likely than for ACC.

In this context, the present study analyzes the performances of the ACC system available in ten market vehicles of different brands, vehicle segments, and powertrains (internal combustion engines, hybrid electric vehicles and battery electric vehicles). The analysis is carried out by testing the ten vehicles for two days during October 2019 in two different testing environments of the ZalaZONE proving ground (Szalay et al., 2019). The study reports i) the main characteristics of the different ACC systems in terms of acceleration/deceleration distributions, response time, and time gap, ii) the string stability and iii) the hysteresis of the traffic flow they compose, and their effect on two traffic externalities, namely iv) energy consumption and v) safety. Considering the variety and number of vehicles involved, the type and number of tests carried out and the different dimensions assessed, the paper places a gravestone on any hope that current market ACC-equipped vehicles may bring real benefits to motorway traffic. On the contrary, it raises significant concern about their possible negative implications to road safety, road capacity, and energy consumption.

During the experiments, the vehicles form a platoon. In the text, the word platoon is continuously used. It is worth mentioning here that this term only refers to the ten vehicles proceeding one after the other in car-following regime, and it has nothing to do with the vehicle platooning use case related to connected and automated vehicles.

The paper is organized as follows. In Section 2, a literature review on the effects of ACC on traffic and related externalities is provided, including reference to previous experimental campaigns. Section 3 describes the methodology adopted in the analysis. Section 4 describes the experimental campaign and Section 5 the results achieved. Finally, Section 6 summarizes the main findings of the study with the implications for the future development of connected and automated vehicles.

## 2. Background on the effect of ACC on traffic flow

The market penetration of ACC-equipped vehicles is constantly increasing along with the interest of researchers worldwide to assess their impact in terms of traffic flow and stability, also because these vehicles are considered as the first proxy of future Automated and Autonomous Vehicles (ACC vehicles are classified as level 1 or 2 driving automation according to SAE International, 2018).

Initially, the expectations of ACC were high: it had to help drivers rest during long distances on highways, avoid rear-end collisions, and decrease traffic jams by impeding hard braking due to harsh maneuvers of other cars on highways, all the while keeping a small, constant time gap after the leading car. Over time, these expectations have been supported by simulation studies attempting to quantify the potential benefits. Marsden et al. (2001), although identifying situations in which ACC vehicles could have led to traffic problems (e.g. vehicles cutting in the ACC vehicle and leading to sudden strong decelerations) on average reported significant comfort and environmental benefits connected to their widespread. Treiber and Helbing (2001) stated that if only 20% of vehicles are equipped with driver-assistance systems, they can eliminate congestion almost completely. Vahidi and Eskandarian (2003), although identifying a possible deterioration of road capacity in the case of large time headways applied to ACC vehicles, supported the idea of smoother

traffic operations enabled by these systems. Davis (2004a, 2004b) showed that ACC can suppress wide moving jams by making the flow string stable. Ioannou and Stefanovic (2005) found that ACC systems can benefit traffic flow and bring positive environmental impacts, dampening traffic disturbances. As mentioned in the work by Xiao and Gao, "People deserve safer, more comfortable and more efficient vehicles and they will get it" (Xiao and Gao, 2010). More recently, car-platoons of ACC systems have been found to reduce frustrating phantom traffic jams (Ford, 2019) and reduce fuel consumption (Zhu et al. 2019).

Soon after the first studies, researchers started raising doubts about the benefits that actual commercial ACC controllers may bring to traffic flow and started defining requirements and proposing alternative control schemes. Zhou and Peng (2005) for example defined a methodology to design the proper range policy of an ACC controller, namely the selection of the desired following distance as a function of the vehicle speed. The paper highlighted the fact that without a proper range policy, the ACC can produce string unstable traffic flow. Martinez and Canudas-de-Wit (2007) defined conditions that guarantee safety and comfort as they realized that these two parameters are very sensitive. Kesting et al. (2007, 2008) proposed an ACC logic able to improve traffic stability and road capacity. Xiao and Gao (2011) highlighted the negative effect that parasitic time delays in ACC controllers have on string stability and underlined the importance of string stability as one of the requirements in the ACC design. Similar recommendations are introduced by Davis (2012), Ploeg et al. (2014), and Farnam and Sarlette (2019) in the design of both ACC and Cooperative ACC controllers (CACC). Other authors have focused on achieving controllers able to guarantee safety and higher fuel efficiency (Han et al., 2018).

It is worth mentioning here that the cooperation enabled by Vehicle-to-Vehicle (V2V) and Vehicle-to-Infrastructure (V2I) communication started to attract considerable attention among researchers as a way to cope with the limitations that researchers started to identify in conventional ACC systems. Several papers on CACC systems have been published in the past years (van Arem et al., 2006; Wang et al., 2018; Shladover et al. 2012; 2015; Dey et al., 2016; Stern et al., 2018; Ge et al., 2018; Ard et al., 2020 just to mention a few), while an increasing number of papers is being published concerning the potential benefits in combining ACC with traffic management strategies (see for example Goñi-Ros et al., 2019; Manolis et al., 2020). Coupling communication with automation, in general, is a widely acknowledged approach to increase the effectiveness of automated mobility systems. However, it adds a significant additional complexity as it requires to exit the vehicle boundaries and define the rules of its interaction with the road transport system. Although from a technical and technological point of view these systems may be almost ready for deployment, from an implementation perspective they will certainly require still a few years.

In recent years, models of ACC and CACC controllers have been used to assess the impact of automated vehicles on motorway traffic. Although AVs will not necessarily operate like ACC or CACC, the lack of data on AVs operations induced researchers to use them as a proxy for AV longitudinal control (see for example Talebpour and Mahmassani, 2016; Mattas et al., 2018; Li and Wagner, 2019). Results achieved are very different and are strongly dependent on the assumptions made to simulate both automated and human-driven vehicles. In most of them, however, connectivity is considered a key requirement to increase road capacity and reduce the string instability of the simulated traffic flow. Similar outcomes are also reported by Tu et al. (2019) which reported high collision risks in car-platoon of automated vehicles lacking V2V communication.

Despite the large number of studies on requirements for ACC systems and their potential impacts, until a few years ago only a minority of studies investigated the properties of systems that are on the market for several years now. Practical difficulties and resources needed to carry out ad-hoc test campaigns are probably among the main reasons for this gap. Among the first studies of this type, Milanés and Shladover (2014) compared the performance of three different controllers, a production ACC, the IDM model, and a proposed CACC controller using test results on four vehicles. The results show that string stability is not achievable for multiple consecutive vehicles using ACC when the leading vehicle speed varies, even under mild speed variations. The instability could be solved through V2V communication, which, as already mentioned, has been suggested to be crucial to achieving the highest possible gains from AVs (Shladover, 2018; Mattas et al. 2018). More recently, Knoop et al. (2019) describe an experiment with seven SAE level-2 vehicles from four makes, driven as a platoon on public roads for a trip of almost 500 km. This experiment showed that the platoon becomes unstable when all vehicles have ACC activated. The speed variations led to discomfort and even risks of rear-end collisions. The most dangerous situations occurred when the leading vehicle had to oscillate its speed (i.e., deceleration followed by acceleration and deceleration). Finally, Gunter et al. (2019) assessed the string stability of seven 2018 model year ACC-equipped vehicles from two makes. All vehicles under all following settings were found to be string unstable.

To fill the lack of experimental data and contribute to clarify the impact of commercially available ACC systems on traffic flow, the Joint Research Centre of the European Commission organized during 2018 and 2019 four test campaigns involving different ACC-equipped vehicles. The campaigns were carried out in different configurations and using different settings to explore several parameters that could affect the ACC operations. Results have been summarized in several papers. In particular, Makridis et al. (2020a) derived the response time and time gap distribution of a commercial ACC system operating at low speed (<60 km/h) and found that both parameters were not significantly different from those commonly reported for human drivers, thus questioning the positive impact of such a system on road capacity. He et al. (2020a, 2020b) reported the results of three tests involving four ACC vehicles driven on public motorways both by the ACC and by human drivers in terms of positive energy demand. From the study, the experiments in which the vehicles were driven by the ACC resulted in requiring more energy than the experiment in which the vehicles were driven by a human driver, questioning the positive impact of ACC vehicles on energy/fuel consumption. Makridis et al. (2020b) investigated the string stability of a platoon of five ACC-equipped vehicles, tested under different conditions in the AstaZero proving ground. Results demonstrated that in all conditions, ACC was string unstable, confirming the findings of the other studies. The data collected in these test campaigns have been used to also draw initial inferences about other implications of the ACC, namely safety and road capacity. To allow the scientific community to further work on these data and to study other aspects of the ACC behavior, the entire database has been made publicly available (Makridis et al., 2021). The authors had the impression that the few electric vehicles involved in the different test campaigns performed comparatively better than vehicles with internal combustion engines, which could be explained by

the faster response that an electric engine can provide. In addition, the behavior of ACC systems from different manufacturers may differ significantly, and the string stability behavior for different speed and time gap settings could differ even for the same controller. Moreover, in Makridis et al. (2020b) the vehicle speed profile was shown to be affected by the altitude changes in the test track without clear indications if this influence could induce instability. Finally, almost all the available experimental campaigns refer to medium/high-speed operations of the ACC, whereas these systems are now able the operate at any speed. To shed light on these additional aspects and to carry out a comprehensive final investigation on the impact of commercially available ACC systems on motorway traffic flow, the present paper summarizes the outcomes of a test campaign involving ten ACC equipped vehicles from different makes and powertrains. Tests were carried out in two test-tracks of the ZalaZone proving ground, as detailed in the following sections.

## 3. Methodological framework

Before proceeding to describe the test campaign and the results achieved, the present section introduces the methodological framework used in the study. Differently from other studies on the same subject, the results of the study are entirely based on the analysis of the experimental data collected during the test campaign and as such are in principle limited to the adopted experimental settings. The authors decided not to use the collected data to calibrate any model of an ACC system for the intrinsic complexity of this task (Punzo et al., 2012) and not to introduce in the analysis the uncertainty linked to the capability of the model to reproduce the actual ACC operating strategy.

### 3.1. Properties of the ACC controller

The core functionality of commercial ACCs is still only marginally understood due to intellectual property rights (He et al., 2019). Four characteristics of the commercial ACC systems are investigated in the present work: the time gap settings, the response time to the actions of the vehicle in front, and the rates of acceleration and deceleration allowed. The parametrization of the controllers based on these four characteristics may directly impact several traffic-related phenomena, and it is of interest for microsimulation modeling and impact assessment studies.

Acceleration and deceleration distributions are drawn using the data collected during the experimental campaign without the application of additional smoothing. Although the existence of outliers is expected, the bulk of the distributions are considered representative of the actual dynamics. Further filtering of the speed signal can affect those distributions and for this reason it was not performed.

The methodology adopted to estimate the time gap values is described in Makridis et al. (2020a). In particular, the target time gap for each vehicle is estimated based on the distributions of the instantaneous time gap values that each vehicle keeps during the experiments. Since the controllers aim at keeping a constant gap, the hypothesis is that the target gap is the median of the observed distribution for each vehicle.

For the estimation of the response time, the methodology described in Makridis et al. (2020a) was also used. The platoons start from steady-state conditions, and a change in the speed of the leading vehicle is the initial input. The corresponding output is on the acceleration of the investigated ACC controller. Consequently, the cross-correlation coefficient between the relative speed and the acceleration of the follower is calculated, while shifting in time one of the two signals. The time shift for which the correlation is
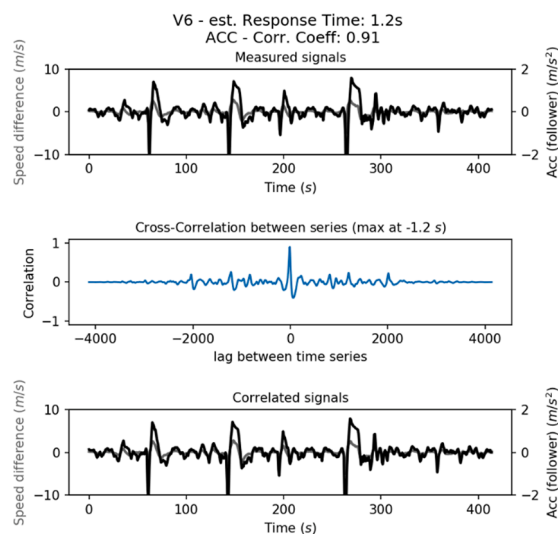


**Fig. 1.** Example of observable response time estimation for an ACC system based on experimental observations. The top figure shows the two series under study (the speed change of the leader vehicle and the acceleration of the follower), the middle figure illustrates the correlation between them and the bottom figure shows the shifted series.

maximum is considered a good approximation of the controller's observed response time. An illustrative example of this procedure is shown in Fig. 1. The two series shown in the top subfigure represent the speed difference between the follower and the leader. Their correlation (middle subfigure) provides a clear peak value, which according to the employed methodology is the estimated observable response time of the controller. The final shifted series are shown in the bottom figure.

### 3.2. String stability

As emerging from the literature review, one of the main motivations of the current work is to investigate the behavior of commercial ACC controllers regarding string stability. String stability is relevant to the introduction and amplification of stop-and-go waves in congested traffic.

There is a vast literature on the string stability of a platoon of vehicles. Significant efforts have been made in investigating the string stability of car-following models (Wilson and Ward, 2011). Understanding the behavior of mathematical constructions like car-following models is important for microscopic traffic simulation and possibly for the design of automated controllers that are beneficial for the traffic flow, as in the work of Wang et al. (2018). Different approaches using the characteristic equation, Lyapunov stability, the direct transfer function-based method, and more have been developed, and a review can be found in the work of Sun et al. (2018). More recently, Montanino and Punzo (2021) showed the equivalence of previous approaches from the traffic flow theory and the control theory domains, and proposed an unfying analysis framework.

In general, after a perturbation in the velocity of a vehicle in a platoon, the perturbation travels upstream, with the following vehicles adjusting their velocity. This deviation from the equilibrium conditions can be measured in the velocity or inter-vehicle distance, using p-norms, which is at the basis of the so-called $L_p$ stability (Feng et al., 2019; Montanino et al., 2021). For any vector $y$ in $\mathbb{R}$, its p-norm can be calculated as in Eq. (1).
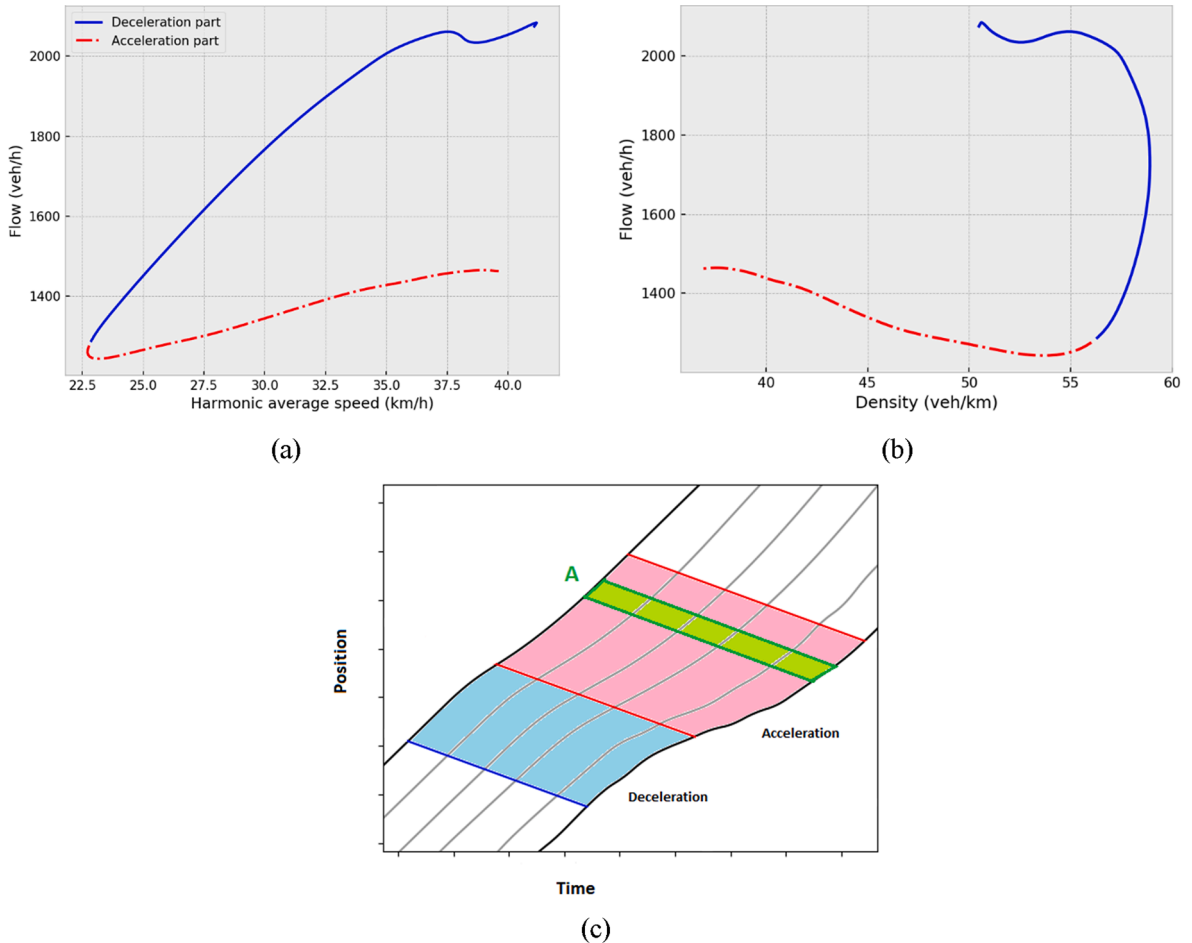


**Fig. 2.** Example of traffic hysteresis in a speed-flow diagram (a), a density-flow diagram (b), and a time–space diagram (c). Deceleration and acceleration phases of the traffic oscillation are highlighted in both charts.

$$\|y\|_p = \left( \sum_{i=1}^{n} |y_i|^p \right)^{\frac{1}{p}}, p \in [1, \infty] \tag{1}$$

In common applications, *2-* and $\infty$-norms are usually used to perform $L_2$ and $L_\infty$ string stability analysis. In particular $L_2$ is related to energy demand, as it refers to the distance between the car-following state and the steady-state conditions for the complete duration of the perturbation scenario. On the contrary, $L_\infty$ considers only the maximum magnitude of the perturbation traveling upstream. This latter relationship is easily demonstrated since the infinity norm of a vector is defined as the maximum of the absolute values of its components:

$$\|y\|_\infty = \lim_{p \to +\infty} [\left( \sum_{i=1}^{n} |y_i|^p \right)^{\frac{1}{p}}] = \lim_{p \to +\infty} [(|y_1|^{\infty p} + |y_2|^{\infty p} + \cdots |y_n|^{\infty})^{\frac{1}{p\infty}}] \tag{2}$$

By raising to the infinite power, the smaller elements of the vector become negligible compared to the maximum one. Therefore, we get:

$$\|y\|_\infty = max\{|y_i| : i = 1, \cdots, n\} \tag{3}$$

In the present work, the $L_\infty$ stability is calculated because it is related to the appearance of stop-and-go waves and vehicle safety. The vector of the disturbance used in all cases is the difference between the velocity of the stable platoon and the actual velocity of each vehicle. If for a platoon the norm of the speed disturbance is for each vehicle smaller than that of the vehicle ahead, there is strict string stability. If instead, the norm of the disturbance of the vehicle after the perturbed vehicle is smaller than that of the last vehicle there is weak string stability (Monteil et al., 2019; Montanino et al., 2021).

A number of perturbation events have been isolated from the data collected, starting and ending with all vehicles having similar velocity. Following the definition of weak and strict string stability and the definition of $L_\infty$, the magnitude of the perturbation of each vehicle is evaluated, and it is compared to that of the second vehicle of the platoon and to that of the vehicle directly ahead. The ratio of the magnitude of the perturbation of a vehicle over the vehicle upstream is calculated in both cases. When the value of the ratio is less than 1, the perturbation of the vehicle downstream is smaller, implying string stability. The two ratios will be referred to as weak string stability indicator and strict string stability indicator, respectively.

### 3.3. Traffic hysteresis

String unstable platoon behavior can be experienced in today's traffic under congested conditions. Stop-and-go waves are formed and travel upstream with increasing magnitude. In these cases, the traffic hysteresis phenomenon is often observed as it is closely correlated to the traffic oscillation (Laval and Leclercq, 2010). For these traffic oscillations, the speed and flow recovery are often delayed, resulting in parts of the platoon with decreased traffic flow. One of the common assumptions for the causation of hysteresis is an asymmetry between the acceleration and deceleration part of the car following behavior (Chen et al., 2014). An example of hysteresis is presented in Fig. 2a, a diagram of the harmonic average speed and the flow, and in Fig. 2b, a density to flow diagram of a platoon of vehicles during an oscillation. The blue line represents the deceleration part and the red one represents the acceleration part of the oscillation. While the vehicles accelerate to recover their platoon speed, the inter-vehicle distances are larger, so the flow of the platoon is decreased for this time.

Some of the key factors in determining the magnitude of traffic hysteresis have been proposed to be the difference in driver aggressiveness, heterogeneity in driving style, or even possible driver distractions (Laval and Leclercq, 2010; Chen et al., 2014; Saifuzzaman et al., 2017). Using the data from the experiment, it is possible to investigate the existence and magnitude of traffic hysteresis generated by an ACC traffic flow to understand the possible impact of ACC-driven vehicles on road capacity and traffic flow stability.

Laval (2011) has developed a method for measuring the magnitude of traffic hysteresis using trajectory data and macroscopic characteristics of the traffic flow, and Ahn et al. (2013) developed a method for measuring it using microscopic characteristics of the traffic flow. The method of Laval (2011) is adopted in this study to quantify the traffic hysteresis and estimate the loss in traffic flow. The traffic variables are evaluated using Edie's generalized definitions (Edie, 1961). For a platoon of $n$ vehicles in a time–space region $A$ so that

$$k = \sum_{i=1}^{n} t_i / |A| \tag{4}$$

$$q = \sum_{i=1}^{n} x_i / |A| \tag{5}$$

$$u = \frac{q}{k} = \sum_{i=1}^{n} x_i / \sum_{i=1}^{n} t_i \tag{6}$$

where the $k$ is the density, $q$ is the flow, and $u$ the speed. $|A|$ is the area of $A$, $t_i$ the travel time and $x_i$ the traveled distance inside $A$, as proposed in Laval (2011). The area $A$ is a parallelogram with a slope equal to a wave speed of 15 km/h in the time–space diagram.

The deceleration and acceleration parts of the traffic oscillations were divided based on the change in the average speed of the platoon. An example is presented in Fig. 2c where a platoon of six vehicles is represented in the time–space domain. Each line represents the space traveled over time by a vehicle. The first and last vehicles are represented by a black line, while the intermediate vehicles are represented by a grey line. The time–space areas of the deceleration and acceleration phase are denoted with light blue and light red colors, respectively. The leading vehicle is not considered in the calculations of density, flow, and speed. Its behavior is controlled, so it is not considered to be a vehicle in the platoon, but an obstacle for the first follower vehicle, to study the behavior of the ACC driven vehicles.

The different perturbations are identified manually in the data, from the velocity profiles of the vehicles, using the relevant notes that the authors kept during the experiments. Then, identifying the areas of deceleration and acceleration and using Eq. (5), the average flow during the deceleration and acceleration phases are calculated. The difference in the average flow is the magnitude of the hysteresis for each perturbation in the experiment. The focus of the present section is on the hysteresis magnitude, which directly estimates the decrease in traffic flow, and not on secondary characteristics that can be interesting for other research purposes, as the duration and intensity of the oscillation (Zheng et al., 2011).

### 3.4. Energy consumption

When approaching the energy impact of ACC driving behavior, the tractive energy consumption is a suitable assessment indicator from a transport engineering perspective (Ciuffo et al., 2018). Although it does not directly reflect the engine fuel consumption or the battery charge depletion, this metric can rule out the energy effect of heterogeneous propulsion systems in the traffic network (He et al., 2020a). In addition, the auxiliary loads are not considered in the computation of tractive energy consumption, but all test vehicles are supposed to use the same auxiliary functions during the test campaign in this study. Specifically, the vehicle's tractive energy consumption ($E_t$, kJ) is calculated by integrating the tractive power demands ($P_t$, W) at the wheels over time (He et al., 2020b), without considering the negative power components from the regenerative braking, as described by:

$$P_t(t) = \max\left\{0, f_0 \cdot \cos\theta(t) \cdot v_e(t) + f_1 \cdot v_e(t)^2 + f_2 \cdot v_e(t)^3 + 1.03 \cdot m \cdot a_e(t) \cdot v_e(t) + m \cdot g \cdot \sin\theta(t) \cdot v_e(t)\right\}, \tag{7}$$

$$E_t(t) = \int_0^T P_t(t) \times 10^{-3} \cdot dt, \tag{8}$$

where $f_0, f_1$ and $f_2$ are road load coefficients (N, kg/s, and kg/m, respectively); $m$ is the vehicle mass (kg); $v_e$ and $a_e$ are speed (m/s) and acceleration (m/s$^2$) of the ego vehicle, respectively; $\theta$ is the road gradient (rad); $g$ is the gravitational acceleration (9.81 m/s$^2$); $dt$ is the time interval (s) between consecutive measurement points; $T$ denotes the total duration (s) of the travel period.

In a platoon consisting of ACC-driven vehicles, the tractive energy consumption of following vehicles is usually larger than that of the leading one because ACC followers, using only local sensors, can lead to string instability and therefore amplify speed perturbations propagating upstream in the platoon. At the individual level, the intra-platoon tractive energy increase ($\delta E_{F/L}^i$, %) of each following vehicle relative to the leading one is defined as:

$$\delta E_{F/L}^i = \left(\frac{E_t^i}{E_t^1} - 1\right) \times 100\%, \tag{9}$$

where $i$ is the vehicle index that increases towards the upstream direction of the platoon; $E_t^1$ and $E_t^i$ are the tractive energy consumption (kJ) of the first (leading) and $i$th (following) vehicles in the platoon.

To further evaluate energy impacts of speed perturbations on the whole platoon (namely, at the platoon level), the average intra-platoon tractive energy increase ($\Delta\overline{E}_{F/L}$, %) is described as:

$$\Delta\overline{E}_{F/L} = \frac{1}{n-1}\sum_{i=2}^{n}\delta E_{F/L}^i, \tag{10}$$

where $n$ is the number of vehicles in the platoon.

On the other hand, this study evaluates the energy performance of different platoons. For example, the tractive energy consumption of platoons with all vehicles set to maintain the shortest time-gap (referred to as S-ACC platoons) is compared with that of platoons in which vehicles may have been set to maintain either the shortest or the longest time gap (SL-ACC platoons) to highlight the energy benefits of mixing short and long time gap ACC systems in the platoon. In this comparison, the inter-platoon tractive energy difference ($\delta E_{SL/S}^i$, %), between two vehicles in different platoons but occupying the same position within the platoon, is presented as:

$$\delta E_{SL/S}^i = \left(\frac{E_{t,SL}^i}{E_{t,S}^i} - 1\right) \times 100\%, \tag{11}$$

In addition, the total inter-platoon tractive energy difference ($\Delta E_{SL/S}$, %) between these two platoons (S-ACC and SL-ACC) is calculated as:

$$\Delta E_{SL/S} = \left( \sum_{i=1}^{n} E_{t,SL}^{i} / \sum_{i=1}^{n} E_{t,S}^{i} - 1 \right) \times 100\%,$$ (12)

### 3.5. Safety implications

Since ACC-driven vehicles already represent a first level of driving automation, it would be expected that they could already contribute to increasing road safety in motorway driving. Indeed, it is argued that ACC can also reduce the frequency of rear-end collisions by keeping a safe distance, quickly reacting to leader vehicle actions, and dampening traffic shock-waves (Li et al., 2017).

As already pointed out, vehicle manufacturers do not have to fulfill any explicit safety requirement in developing their ACC systems (nor demonstrating that ACC vehicles have to dampen traffic oscillations), which are considered systems aimed at increasing driving comfort and requiring constant supervision by the driver. At the same time, several studies have shown that over time drivers tend to increasingly trust the robustness of the ACC systems and start to divert their attention towards secondary, non-driving related tasks (see for example De Winter et al. 2014). This has recently reached the attention of the general public due to the crashes caused by improper use of different level 2 automated vehicles (BBC news, 2020). Furthermore, Makridis et al. (2020b, 2020c) have shown potential safety issues in platoons of ACC-drive vehicles due to their capability to amplify the magnitude of traffic oscillations. As an increasing number of ACC vehicles is in the fleet, the probability of having platoons of ACC-driven vehicles on the road is increasing accordingly and it is, therefore, worth investigating the possible negative effects on safety.

In the experiments carried out for the present study, there have been no crashes. However, in several cases, either the drivers or the automated emergency braking had to intervene to prevent possible crashes. However, the decision to intervene can be an excessive caution by the driver or a conservative setting in the AEB system, hence, it cannot be a useful basis for comparison. To assess objectively whether the experiments generated actual collision risks, traffic conflict techniques are used (Laureshyn et al., 2010). In particular, one of the most widely used surrogate safety metrics, the Time To Collision (TTC), is adopted in the present paper (Laureshyn et al., 2016; Mahmud et al., 2019). The value of TTC for a pair of vehicles, a leader and a follower, can be calculated only when the velocity of the follower is larger than that of the leader. Otherwise, the situation is regarded as safe. When the follower is faster, the TTC calculates the time left until a collision occurs, in the hypothesis that both vehicles continue with constant velocities (Eq. (13)):

$$TTC = \frac{d}{V_{follower} - V_{leader}}$$ (13)

In the equation, $d$ is the inter-vehicle distance, $V_{follower}$ and $V_{leader}$ the velocity of the follower and leader vehicle, respectively. The smaller the TTC value, the shorter the time the following vehicle has to react, and the bigger the risk of an actual collision. The threshold values of TTC proposed in the literature to discriminate between safe and unsafe traffic situations vary from 1.5 to 4 s (Mahmud et al., 2019).

## 4. Case study

The present section describes the experimental campaign carried out for this study. This involves a description of the proving ground, including the track segments where the experiments took place, of the test vehicles, the testing conditions, and introduces the data collection and post-processing of the measurement data.

### 4.1. ZalaZONE proving ground

The experimental campaign has been carried out on the Dynamic Platform and the Handling Course of the ZalaZONE proving ground, in Hungary. Three parts can be identified within the Dynamic Platform: the acceleration section, the circular plate where measurements are carried out, and the connected return road. The diameter of the test area is 300 m and the surface has a maximal 1% inclination. The Handling Course, on the other side, includes curves and inclinations, providing a diverse test environment. A detailed description of the proving ground and the two different test tracks used are provided in Annex 1 reported in the Supplementary Material.

### 4.2. Experimental campaign

#### 4.2.1. Vehicles
The experimental campaign involved 10 vehicles moving in platoon formation behind a leader programmed to follow a specific speed profile. The platoon is a combination of distributed driving systems, in which each vehicle can be operated by either a human driver (HD) or an ACC system. Furthermore, the ACC system can adopt different time gap settings such as short, medium, and long. Consequently, the platoons examined in this paper have the following different configurations of driving systems:

- HD platoon: all following vehicles are human-driven.
- L-ACC platoon: all following vehicles adopt long time gap ACC systems.
- M−ACC platoon: all following vehicles adopt medium time gap ACC systems.
- S-ACC platoon: all following vehicles adopt short time gap ACC systems.

**Table 1**
Basic specifications of vehicles used in the tests with indication of the corresponding code and color notation used in the paper's Figures.

| Brand | Model | Max power (kW) | Drive-Fuel | Engine displacement (cc) | Propulsion type | Battery capacity (kWh) | Top speed (km/h) | ADAS Function | Model year | Code | Color notation |
|---|---|---|---|---|---|---|---|---|---|---|---|
| Tesla | X | 386 | electricity | – | BEV* | 90 | 250 | ACC + AEB + SAS + LSS* | 2016 | V1 | |
| Tesla | 3 | 250 | electricity | – | BEV | 79 | 250 | ACC + AEB + SAS + LSS | 2019 | V2 | |
| Tesla | S | 244 | electricity | – | BEV | 75 | 225 | ACC + AEB + SAS + LSS | 2018 | V3 | |
| Mercedes-Benz | GLE 450 4Matic | 270 | gasoline | 2999 | HEV* | 31.2 | 250 | ACC + AEB + SAS + LSS | 2019 | V4 | |
| Jaguar | I-Pace | 294 | electricity | – | BEV | 90 | 200 | ACC + AEB | 2019 | V5 | |
| BMW | I3 s | 135 | gasoline | 647 | HEV | 33.2 | 160 | ACC + AEB | 2018 | V6 | |
| Audi | E-tron | 300 | electricity | – | BEV | 83.6 | 200 | ACC + AEB + SAS + LSS | 2019 | V7 | |
| Toyota | Rav 4 | 115 | gasoline | 2487 | HEV | 41.8 | 180 | ACC + AEB | 2019 | V8 | |
| Mazda | 3 | 96 | gasoline | 1998 | ICE* | – | 197 | ACC + AEB | 2019 | V9 | |
| Audi | A4 Avant | 140 | gasoline | 1984 | HEV | 0.69 | 238 | ACC + AEB | 2019 | V10 | |

*BEV: Battery Electric Vehicle, HEV: Hybrid Electric Vehicle, ICE: Internal Combustion Engine, ACC: Adaptive Cruise Control, AEB: Automatic Emergency Braking, SAS: Substation Automation System, LSS: Lane Support Systems.

- **SL-ACC** platoon: following vehicles adopt short or long (mixed) time gap ACC systems.

The 10 vehicles have been rented for this experimental campaign. They are all market vehicles with the highest equipment level of ADAS systems. Table 1 reports the specifications of all the vehicles involved in the campaign along with their code names and color scheme used in the figures of the paper. In addition to them, two target vehicles have been used, namely a robotized Smart (BME ADdv) in the Dynamic Platform and a Skoda Octavia in the Handling Course. In the Figures, they are indicated with black color. In the remainder of the paper, each vehicle will be referred to with the corresponding code according to Table 1.

Experiments carried out in the Dynamic Platform involved a specific speed profile for the target vehicle. This Target vehicle was developed by the Budapest University of Technology and Economics (BME) with the capability to fulfill the dynamic and accuracy requirements of such measurements with its longitudinal control algorithm based on fuzzy systems (Bogya et al., 2019). More information can be found in Annex 1 reported in the Supplementary Material.

All vehicles in the platoon applied the same target speed to their ACC system (100 km/h) and all the drivers were instructed not to disengage the ACC unless a safety–critical situation required it. In cases of malfunctioning of the ACC systems or on the data collection system of a specific vehicle, the affected vehicles were instructed to leave the platoon formation. The experiment would continue without the vehicle, and the vehicle could not join until the end of the ongoing experiment. Therefore, in the results section, it can be observed that the number of vehicles in the platoon varies for different experiments. In addition, human-driven (HD) platoons only serve as a benchmark against various types of ACC platoons. To avoid complicating the comparisons, human drivers in HD platoons were instructed to follow their typical driving pattern (to be neither aggressive nor passive) in urban areas and attempt to close any widening gaps in front of their vehicle. In addition, the drivers would be warned via radio communication when there are possible safety–critical situations at downstream locations, which to some extend can homogenize the driving behaviours of less and more experienced drivers.

The trajectories of the vehicles under test were collected using 2 independent GNSS systems for redundancy. Further technical details on the campaign design and the data processing are presented in Annex 2 reported in the Supplementary Material.

It is worth mentioning that the final version of the dataset is part of the JRC openACC database (Makridis et al., 2021) reporting the results of several experimental campaigns involving ACC vehicles.

### 4.2.2. Day 1 - dynamic platform

As already mentioned, in the Dynamic Platform, the leading vehicle was the BME ADdv. The vehicle was programmed to follow a specific speed profile, while the other vehicles followed the leader in predefined orders using the ACC. Starting for quasi steady-state conditions, where all vehicles had almost the same constant velocity, the Target vehicle decelerates at a target deceleration of $-3 m/s^2$, reaches a predefined lower speed, and then accelerates with an acceleration value of $1 m/s^2$ until it reaches the initial speed again. Fig. 3a illustrates an example test sequence, with three different target equilibrium speeds of 40, 50, and 60 km/h and several perturbations of different magnitude.

Several test runs were carried out with 4 different vehicle orders using short, medium, and long time gap settings. Table 2 presents a general overview of the tests performed in the Dynamic Platform. Unfortunately, the tests could be carried out only with a target speed of 30 and 40 km/h and could not reach 60 km/h as originally planned. For higher speed, the lateral forces jeopardized a correct execution of the tests with several vehicles deactivating the ACC system after a few minutes of testing. A picture taken from the test performed on the Dynamic Platform is reported in Fig. 3b. More details on the test execution can be found in Annex 2 reported in the Supplementary Material.

### 4.2.3. Day 2 - Handling course

In the Handling Course, the leader vehicle was the Skoda (Target), using the cruise control system to keep a constant target velocity. Fluctuations of the Target vehicle velocity shown in Fig. 4a are only caused by the road geometry and the capability of the CC to maintain the constant desired velocity. A picture taken during the experiment is presented in Fig. 4b. Tests were carried out for 30, 50
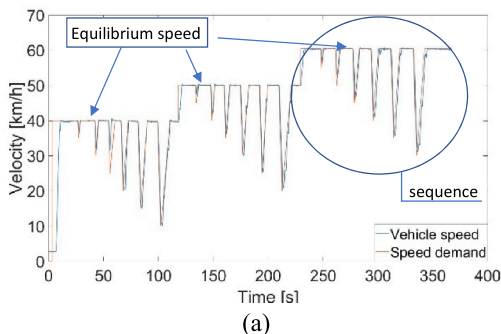


(a)                                             (b)

**Fig. 3.** Experiment settings on the Dynamic Platform. Target speed profile (and actual speed) for the leader vehicle in a test-sequence (a) and a picture of the entire platoon during the tests (b).

**Table 2**
Overview of the parameter variations in the experiments carried out on the Dynamic Platform.

| Equilibrium Speed (km/h) | Perturbation- final speed (km/h) | Time gap settings | Number of vehicle orders |
|---|---|---|---|
| 30 | 25, 20, 15 | Long, short, medium | 4 |
| 40 | 35, 30, 25, 20, 15, 10 | Long, short, medium | 4 |
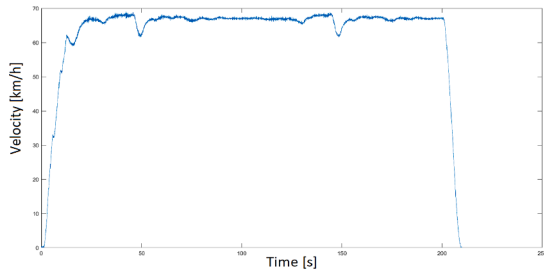


(a)            (b)

**Fig. 4.** Experiment settings on the Handling Course. Speed profile of the leader vehicle in a test-sequence (a) and a picture of the entire platoon during the tests (b).

and 60 km/h and using both the longest and shortest time gap setting. In addition, experiments were also performed with a mix of different time gap settings, with the whole platoon using under the shortest time gap, with the exception of the two central vehicles that used the longest. Experiments with manual driving were carried out as well. An overview is presented in Table 3.

## 5. Results

The present section summarizes the results from the experimental campaign following the methodology described in Section 3. In addition to them, a section dedicated to the lessons learned during the experimental campaign is also reported in the Supplementary Material (Annex 2) for the reader's convenience. From those insights, the difficulty of achieving steady-state conditions, even in the Dynamic Platform, is considered to be significant for properly understanding the paper's results and is described in the next subsection.

### 5.1. Steady-state conditions on the dynamic platform

It was extremely difficult and time-consuming to stabilize the platoon before applying a perturbation in all tests on the dynamic platform. Fig. 5(a) shows an example of the platoon speed profile between two perturbations, where continuous oscillations of the vehicle speed can be observed. The legend refers to the vehicles, according to Table 1.

Fig. 6 shows the root mean square deviation (RMSE) between the target speed (in the case of the figure it was 30 km/h) and the actual speed achieved by each vehicle in the platoon for two time gap settings. The RMSE is calculated both considering the whole measurement (thus including the perturbation) and the portion of the speed profile where the platoon is supposedly in steady-state (thus labeled as RMSE steady-state). The average deviation increases with the position of the vehicle in the platoon, which is already an indication of what will be discussed in the remainder of the text about the string stability of the ACC controller.

From what the authors could observe, the reason for these continuous oscillations may be related to two factors. First of all, the drivers had to apply small continuous manual corrections to the steering wheel. Small deviations in the steering angle can initiate small speed oscillations. Another presumable factor is the inclination of the Dynamic Platform (in the order of 1% to limit the accumulation of water on the surface). The altitude variation over the dynamic platform translates into a variable force applied to the vehicles while completing the circle, which, considering the low speed of the experiments, s comparable with the rolling and aerodynamic resistance and is, therefore, able to disturb their motion. Indeed, the sinusoidal shape of the slope experienced by the vehicles, as showed in Fig. 5 (b), is compatible with the periodicity of the oscillations in the speed profile of the target vehicle.

**Table 3**
Overview of the parameter variations in the experiments carried out on the Handling Course.

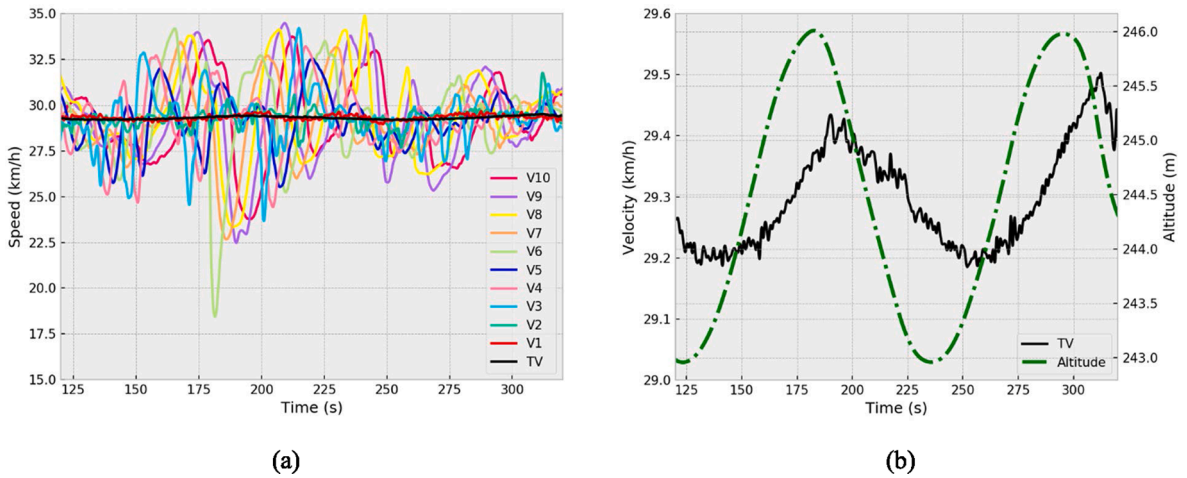| Constant Speed (km/h) | Settings | Number of laps | Number of vehicle orders |
|---|---|---|---|
| 30 | Long, short, mixed time gap, manual driving | 2 | 3 |
| 50 | Long, short, mixed time gap, manual driving | 2 | 3 |
| 60 | Long, short, mixed time gap, manual driving | 2 | 3 |

**Fig. 5.** (a) Example of speed profile for the vehicles involved in the tests on the dynamic platform (platoon with vehicle set to keep a long time gap) without speed perturbations by the leader. (b) Speed profile of the Target Vehicle and Altitude change.
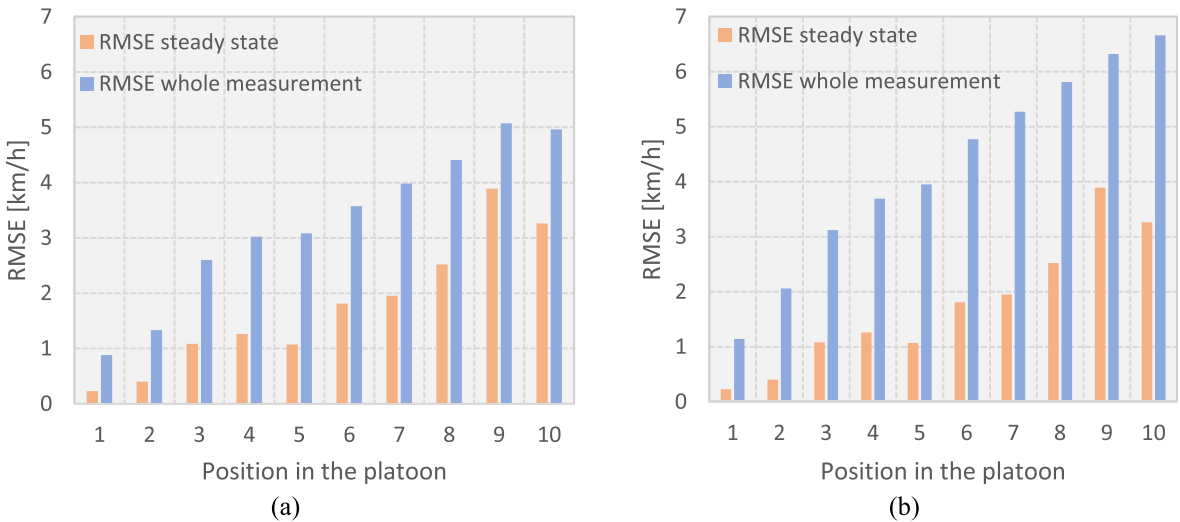


**Fig. 6.** Root mean square deviation (RMSE) of the vehicle speed from the target speed for a whole experiment with target speed of 30 km/h both with the vehicles operating with the longest time gap (a) and with the shortest one (b). Different bars refer to the RMSE calculated using the whole measurement or the speed profile of the platoon before the perturbation.

### 5.2. Properties of the ACC controller

The results presented in this section provide an overview of the main properties of the commercial ACC systems under test. The main goal is to provide deeper insights on how these systems operate and estimate two important parameters, the time gap setting and the response time, as they are crucial in understanding the potential impact on traffic flow, safety, and capacity of these systems.

The dataset has been divided into 340 partial car-following trajectories of at least 10 s duration each. Each of these trajectories refers to a pair of vehicles in car-following. Additionally, the analysis takes into account the test track where the test has taken place (since the two tracks have different characteristics), the position of the vehicles in the car-platoon (2nd to 11th), the desired gap setting by the driver (i.e. small, medium or large), the model/brand of the vehicle and whether the ACC was enabled or not.

The first investigation regards the acceleration and deceleration distributions of HD and ACC platoons. The results suggest that for ACC, the average acceleration and deceleration values are smaller in absolute value, suggesting that for steady-state, there is less variation in speed when the ACC is on. However, outliers are quite consistently higher for the ACC case, especially for the deceleration values. This can be attributed to the behavior of the ACC during perturbations, that provokes harder decelerations as in many cases safety–critical situations arise. This assumption is further supported by the results of the string stability and safety investigations that will be presented in the next sub-sections. More information is reported in Annex 3 of the Supplementary Material.

Fig. 7 shows the main results of the time gap study. According to the literature (He et al., 2019), the control logic in commercial
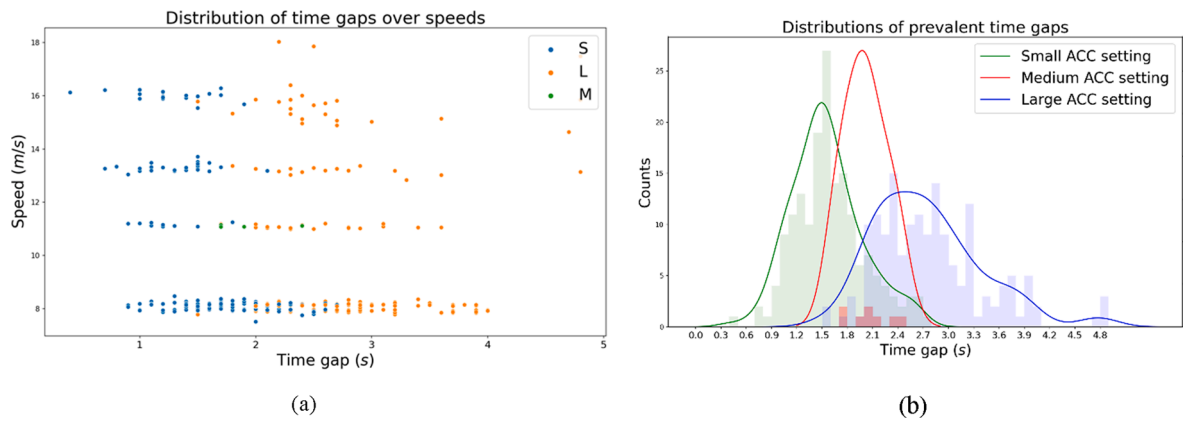
**Fig. 7.** Distributions of the estimated time gap for the vehicles involved in the experiments. Chart (a) shows the measured time gap over different speeds per different time gap settings, while chart (b) shows the time gap distribution per each settings accross the whole experimental campaign.

ACC systems is designed based on the time gap with the vehicle immediately in front. The user sets a desired distance setting (usually noted abstractly, i.e. 1–4 or low, medium, large) and a maximum desired speed. The controller reflects these choices to a time gap strategy from the leading vehicle or a free-flow strategy close to the desired speed in its absence. Consequently, Fig. 7a reflects the prevalent (filtered based on median values) time gap operational values for the systems. The prevalent time gap values refer to large trajectory parts on stable speed conditions (ideally equilibrium conditions). From the speeds (y-axis) and the time gap values (x-axis) one can easily derive the corresponding distances in meters. The variance within the same time gap cluster are due to the different vehicle brands and models. The vehicle order in the platoon did not appear to play an essential role although it is possible that some ACC system could use the information of more vehicles ahead and thus adapt the distance to the vehicle in front accordingly. Finally, Fig. 7b illustrates the unfiltered instantaneous time gap values as they are observed in the measurements. This latter thus gives an illustrative representation of the operational time gap domain when the ACC system is enabled.

Fig. 7a is the scatter plot of the time gap from the 340 partial trajectories. The x-axis corresponds to the estimated time gap, while the y-axis to the median speed of the partial trajectory, aiming to show if any correlation between the behavior of the controller and the actual speed of the vehicle exists. The experiments refer to four main speeds, 30 km/h, 40 km/h, 50 km/h, and 60 km/h, as it is obvious from the horizontal layout of the points.

Each time gap setting is colored differently. As already mentioned, unfortunately, only a few points refer to the medium setting in the dataset. Interestingly, the operational domain for the gap of the vehicles changes with the speed. At 30 km/h the short time gap setting (blue dots) can have gap values of more than 2 s, and the large time gap setting can reach values over 4 s. As the speed increases,
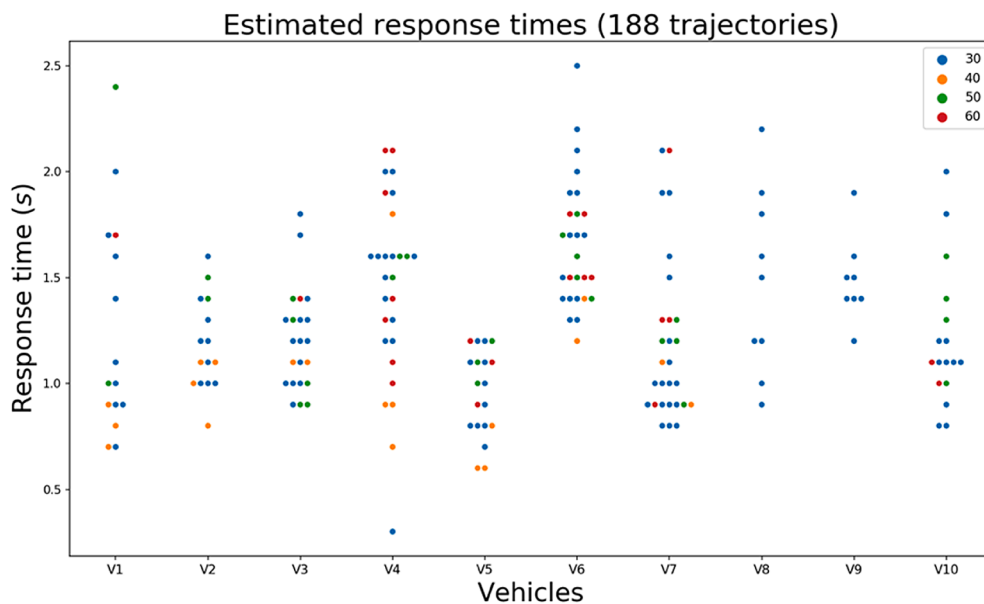


**Fig. 8.** The estimated observed response times for the 10 following vehicles involved in the campaign (independently of the vehicle order inside the platoon). Colors depend on the target speed of the experiment (expressed in km/h).

the variation in the measured time gap is reduced accordingly. Fig. 7b shows the distributions for each of the three settings, showing that the large time gap setting has a much wider distribution than the other two. More details on the acceleration and time gap characteristics can be found in Annex 3 of the Supplementary Material.

Finally, the response time estimations are shown in Fig. 8 per vehicle. The estimation is performed based on the methodology proposed in Makridis et al. (2020a) and briefly described in Section 3.2. This is a correlation-based methodology, which assumes that the trajectories under study refer to (initially) stable conditions. Each estimated response time per pair of trajectories is associated with a correlation value that can be considered as a degree of confidence for the estimation. As it can be inferred, not all estimations can be considered reliable. Therefore, a final post-processing stage took place in order to filter out possible outliers. The estimated observed response times are filtered based on the heuristically-defined correlation threshold of 0.7, where 1 indicates absolute correlation. Specifically, for this study, further visual inspection on the correlated trajectories was performed before the presentation of the final outputs.

Consequently, after the post-processing workflow described above, 152 of the extracted 340 partial trajectories have been discarded since they did not include enough interactions between the two vehicles (follower and leader) in order to provide a good correlation coefficient value and accurate estimation for the response time. In the figure, the different dots are colored on the basis of the experiment target speed. It can be observed that there is no correlation between the different response times and the desired speed (points appear randomly along the y-axis). Vehicles employ different strategies, and it can be assumed that a response time between 1 s and 1.5 s can be representative for commercial ACC systems

### 5.3. String stability

The experiments in the dynamic platform have a conventional structure, similar to the simulation experiments in the work of Sun et al. (2018). From the data, 33 distinct perturbations have been identified and isolated. Each perturbation starts with the platoon in quasi steady-state, as the oscillations in the vehicles' velocities are small compared to the induced perturbation (as mentioned in the
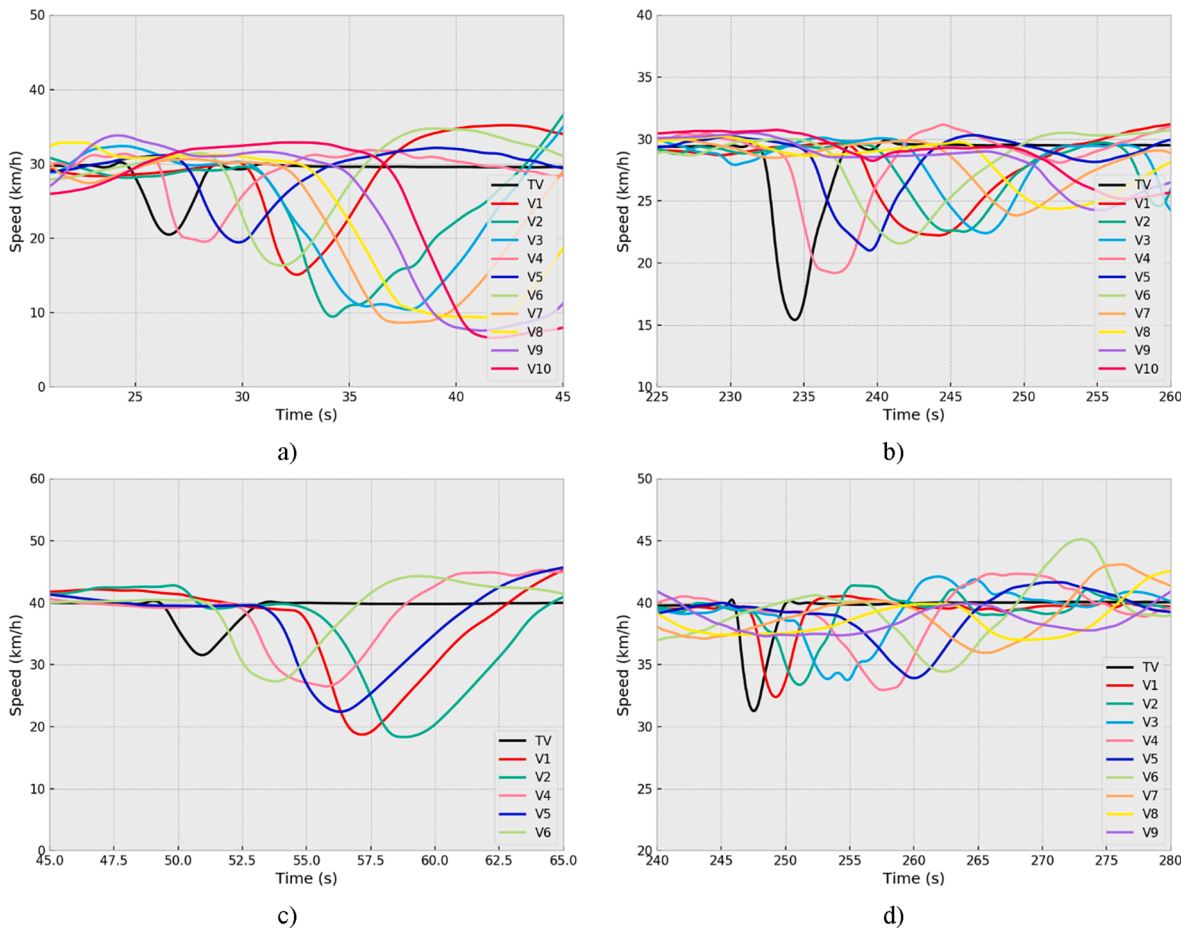


**Fig. 9.** Speed profile of the platoon resulting from four different perturbations during the experiments on the dynamic platform. Charts a) and b) refer to experiments with 30 km/h target speed, while charts c) and d) refer to experiments with 40 km/h target speed. Charts a) and c) refer to experiments with vehicles adopting a short time gap for their ACC, while charts b) and d) to long time gap.

previous section achieving a true steady-state was difficult).

The experiments in the handling course are instead different. There is no induced perturbation in the leader vehicle's speed. The external input to the platoon is the effect of the road geometry on the leader's ACC. It has already been presented in previous work that the ACC controllers can be affected by the slope and curvature of the road (Makridis et al., 2020b). Hence, the road geometry influences the velocity of the leader vehicle creating a small speed oscillation. Thus, the ACC controllers of the follower vehicles react to this oscillation. At the same time, road geometry affects the movement of the follower vehicles as well. Hence, there is a continuous external influence that directly affects all vehicles in the platoon, while each one reacts to the perturbation of its leader's velocity as well. This is different from the experiments in the dynamic platform where there is one measured input to the velocity of the leader vehicle and no direct external influence on the movement of the follower vehicles. One of the main motivations to carry out this experiment was to show that road geometry alone, combined with string instability of the platoon can induce stop-and-go waves. 43 road-geometry induced perturbations have been identified and isolated from the handling course data.

In the next sections, results are reported per test-track used in the experiment.

### 5.3.1. Dynamic platform

Following the methodological framework presented in Section 3 to study the string stability of the platoon, dynamic platform experiments have shown that the platoon of 10 ACC vehicles can either be string stable or string unstable (using the weak string stability definition) depending on the time gap setting applied by the vehicles. Fig. 9 shows examples of the effect of different perturbations on the platoon's speed profile. The labeling in the legend refers to the vehicle model, according to table 1. The leading vehicle is always the TV. For the rest, the further upstream a vehicle is, the later it is affected by the perturbation. Hence, the order can be deduced. For example, in Fig. 9a, it starts with TV, V4, V5, V6, V1, etc. When the vehicles' ACC adopt a short time gap (Fig. 9a, c), the magnitude of the perturbation increases over the platoon. On the contrary, for most cases with the long time gap setting (Fig. 9b,d), the magnitude of the perturbation is attenuated over the platoon. This is consistently experienced independently from the target speed and the vehicles' order in the platoon.

Considering the effect of the time gap setting on the string stability of the platoon, a series of tests with a medium time gap was also carried out. Results of these tests confirm that for the specific type of experiment there must be a critical time gap for which the perturbation magnitude moves unchanged over the platoon. Fig. 10 shows the results of a test with the medium time gap for which indeed the magnitude of the perturbation is only slowly attenuated along the platoon.

To summarize the results of all the experiments carried out, Fig. 11 shows the evolution over the platoon of the median of the distribution of the weak stability indicator presented in Section 3.3 resulting from the experiments carried out in the dynamic platform. Results are shown for the different time gap settings adopted by the ACC systems. The figure confirms the aforementioned correlation between the time gap setting and the string stability of the ACC. In particular, the median value monotonically increases over the platoon for the short time gap, it monotonically decreases over the platoon for the long time gap and remains fairly constant for the medium time gap. It is interesting to notice that the median value of the weak stability indicator for the last vehicle in the long time gap setting is close to 0.5, indicating that the magnitude of the perturbation has decreased almost to half from the second vehicle to the last vehicle. On the contrary, for the shortest time gap setting, the magnitude of the perturbation has more than doubled, moving from the second vehicle to the last in the platoon.

It is also very important to notice that the above results do not depend on the specific vehicle or ACC logic as the results for each position in the platoon are a combination of the outcomes for all the vehicles tested in that position. In this light, the results can be considered general of the ACC logic used in the vehicles on the market and not related to the implementation choices by the different vehicle manufacturers.
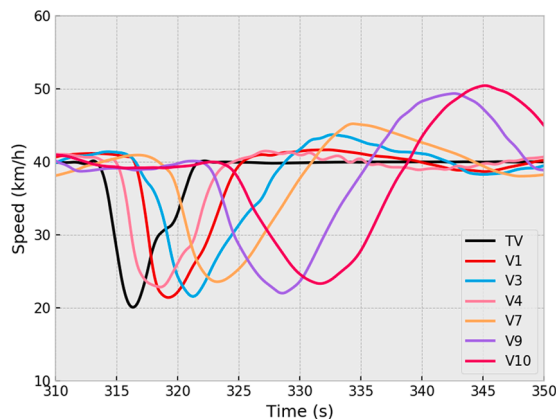


**Fig. 10.** Speed profile of a platoon adopting a medium time gap setting for the ACC as resulting from a 20 km/h perturbation from an initial speed of 40 km/h.
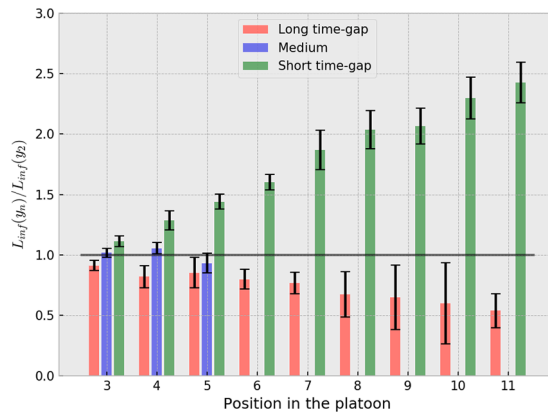
**Fig. 11.** Median weak stability indicator and interquartile range aggregated over time gap selection and position of the vehicle in the platoon in the dynamic platform.

### 5.3.2. Handling course

In the handling course experiments, the source of the perturbations is the road geometry. The shape of the test track is presented in Fig. 12, with each section colored according to the average speed of the first following vehicle in Fig. 12(a) and the last vehicle in Fig. 12(b) during one specific experiment with 30 km/h target speed. The direction of the platoon is counterclockwise, as shown by the blue arrow indicator. While there have been some instabilities throughout the track, the most significant point of concern is a point marked with an "x" which is also the end of a downhill slope and the beginning of an uphill slope. The change in slope generates a deceleration followed by an acceleration to approach the target speed again. This speed variation propagates and amplifies over the platoon. As a result, the last follower has a more turbulent speed profile, increasing to higher speeds and decreasing to lower speeds. Moreover, the point of deceleration and the point of acceleration have moved upstream for the last follower, showcasing standard traffic shockwave characteristics.

Experiment results in the proximity of this perturbation are reported in Fig. 13. In particular, the figure shows speed profiles, space–time diagrams, and oblique space–time diagrams from two experiments, one with the ACC set to the maximum time gap (the three charts on the left) and one to the minimum time gap (the three charts on the right). The oblique plots represent the trajectory of the vehicles, subtracting the average speed, for better readability. The speed profiles (Fig. 13a,b) show that even before the perturbation induced by the slope change, the platoon was not in steady-state conditions as a result of the other, minor perturbations induced by the road geometry (mainly due to the curves). The black line indicates the speed profile of the platoon leader, which uses the cruise control system to keep a constant speed. The velocity of the target vehicle is remarkably stable, showing that the slope change has no significant effects on a single-vehicle velocity. Hence, the observed dynamics are the result of the combined effect of road geometry and string instability.
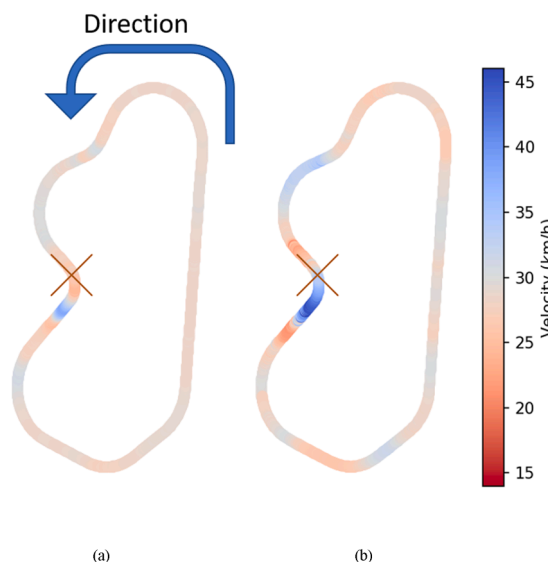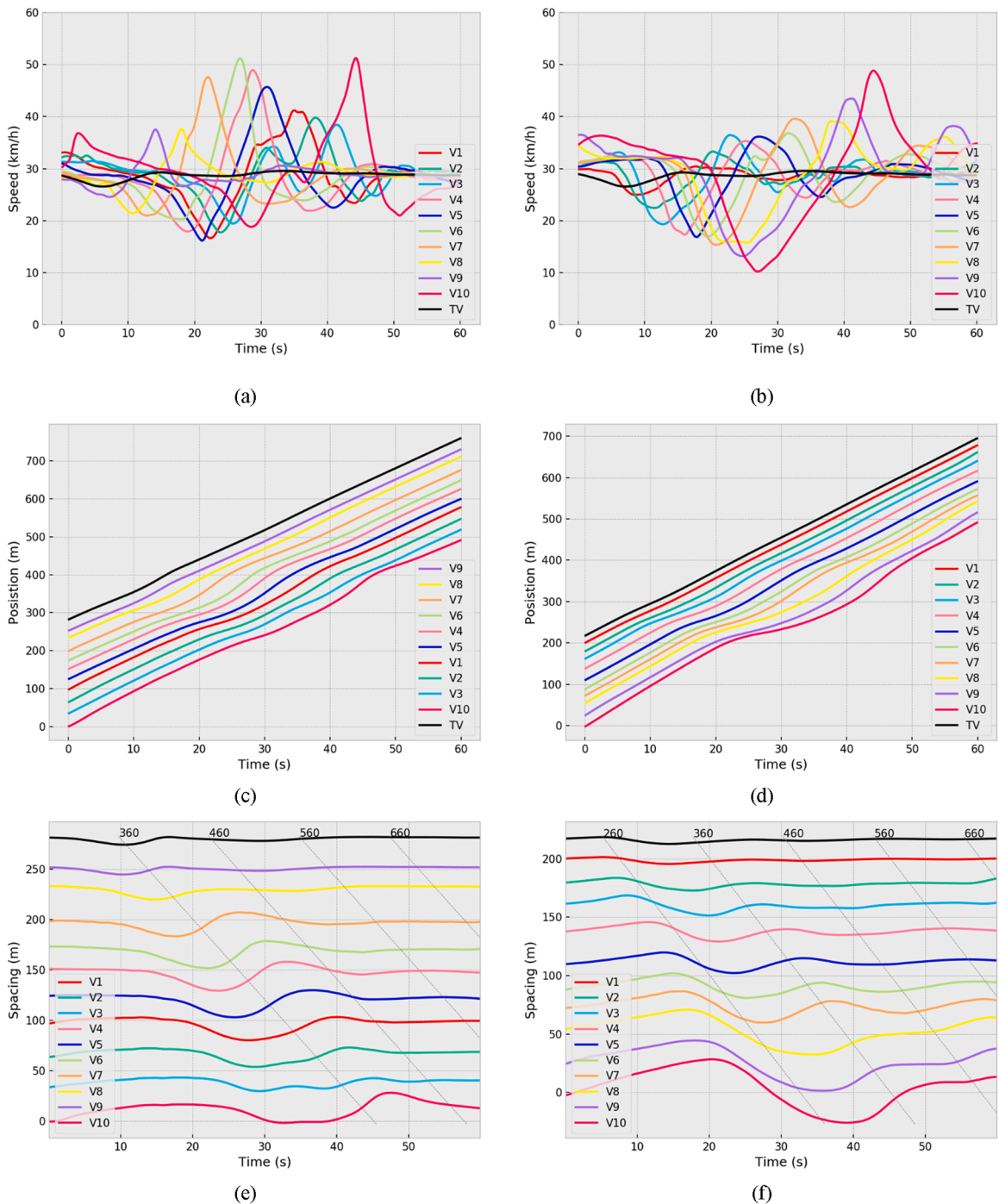


(a)                    (b)

**Fig. 12.** Average speed in the test track for the second (a) and the last vehicle (b).

(a)

(b)

(c)

(d)

(e)

(f)

**Fig. 13.** Speed profiles (a,b), trajectory plots (c,d), and oblique trajectory plots (e,f) for experiments with long time gap (charts on the left) and short time gap (charts on the right).

Before proceeding with the discussion of the results achieved, it is worth noticing that, for the long time gap scenario, it is observed that from the fifth vehicle on, the vehicles accelerate to very high speed. Given the long distance between the vehicles in this scenario, indeed, since the point of slope change is followed by a curve, the last vehicles in the platoon started to lose their leader vehicle, thus accelerating to reach their own target speed (set higher than the experimental speed). This was clear from the vehicle's dashboard indicating the absence of a vehicle ahead during this strong acceleration phase. Since this is not an attribute of the ACC but is due to a combination of the sensor range and the road geometry, the authors have chosen not to take those accelerations into account and to limit the string stability analysis to the deceleration phase only.

The perturbation is amplified for the first vehicles in the platoon in both the long time gap and short time gap scenarios. Only for the last vehicles in the long time gap scenario, the magnitude of the perturbation is attenuated. For the short time gap case, the final vehicle had to decelerate to almost 10 km/h when the first vehicle decelerated only to 26 km/h. The evolution of the perturbation is also apparent from the trajectory and the oblique trajectory plots. The effect on the inter-vehicle distance is also shown in the oblique plots, with the last two vehicles of the short time gap platoon coming very close during the initial deceleration.

The aggregated results of the weak stability indicator for the handling course are presented in Fig. 14. The figure shows the results for the three experimental settings, namely all the ACCs with the minimum time gap, all the ACCs with the longest time gap, and a mixed scenario in which the two central vehicles (position 5 and 6 in the figure) use the longest and the rest use the shortest time gap. The results are different from the experiments in the dynamic platform. For the handling course, the perturbation is induced by road geometry and it directly influences all the vehicles in the platoon. The median of the weak stability indication is always greater than 1. Hence, the magnitude of the perturbation is increasing when traveling downstream and there is no string stability, even for the case of the longest time gap. However, the long time gap platoons in the handling course were less unstable than the other configurations and after the first vehicles in the platoon that showed comparable instability than the vehicles with the short time gap, the remaining vehicles showed that the ACC did not amplify the perturbation's magnitude.

Keeping one or two vehicles with the longest time gap setting in the middle of a platoon of vehicles using the shortest time gap setting showed some slight benefit, especially for the vehicles that are close to those who use the long time gap.

The shortest time gap selection produced the most unstable platoons again. The value of the weak stability indicator is, on average, larger than in the dynamic platform experiments, even for the first vehicles in the platoon. Therefore, the platoons are detected to be more unstable in the handling course part of the experiment.

In the long time gap experiments, it is observed that the magnitude of the perturbation is sharply increasing for the first vehicles in the platoon. For the second half of the platoon, the perturbation does not increase as consistently, as shown in Fig. 13(a) and 14. A possible explanation is that the perturbation is traveling upstream in space so that the vehicles at the end of the platoon are confronted with the perturbation in a different position, thus the effect of the road geometry is different. To further show this point, the long time gap case of Fig. 13(a) has been further investigated. The speed profiles of the vehicles are presented in Fig. 15. This time, however, the speed profile is related to the distance and not to time, as in Fig. 13(a). Also, in the figure, the altitude of each point is indicated by the dotted grey line.

The part of the altitude that affects the speed of the leader vehicle is immediately after position 300 m, where the slope of the road changes from downhill to uphill. However, the last vehicles in the platoon are affected by this perturbation before they reach this part of the test track. In particular, V5 is the first vehicle in which the perturbation is entirely in the downhill part and for the vehicle upstream, the magnitude of the perturbation is significantly attenuated. This observation supports the intuition that for the long time gap case, the instability rises as a combination of the effect of the leader's speed perturbation and the geometry of the road in the position in which each vehicle encounters the propagated perturbation. Further experiments would, however, be needed to study this aspect in more detail.

### 5.3.3. Discussion

Given the potential implications of the results from the string-stability analysis, the present section provides a first discussion. Results indeed leave no doubts on the string-stability of commercial ACC controllers. It confirms the finding of Makridis et al. (2020b, 2020c) and other literature studies. Electric vehicles did not show differences in terms of string-stability as originally considered in preparing the test-campaign and the fact that in conditions closer to real-life, all time gap settings show string-instability and provide a final proof about the properties of the ACC controllers. It has to be said that differently from the existing literature, large time gap platoons tested in a flat test track with constant curvature showed weak string stability, suggesting that by defining a lower bound to the time gap of ACC controllers, traffic shockwaves can be dampened by these systems. One may wonder though, which is the effect on
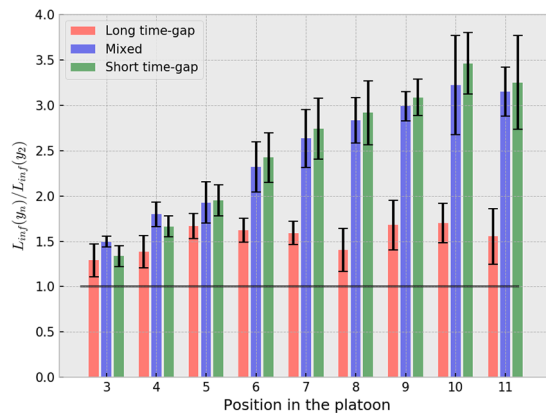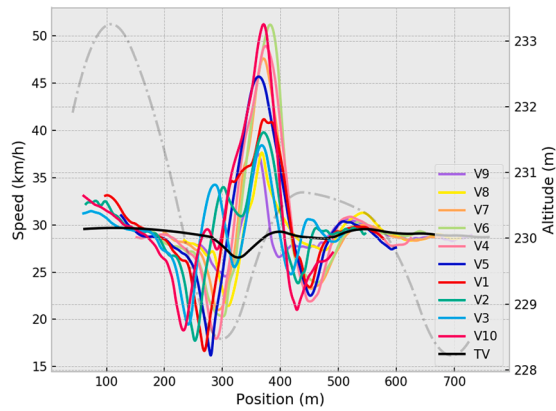


**Fig. 14.** Median weak stability indicator and interquartile range aggregated over time gap selection and position of the vehicle in the platoon during the handling course experiments.

**Fig. 15.** Distance-based speed profile of a long time gap case, plotted against the position. On the second axis, the altitude value is shown, denoted by the black dotted line.

road capacity of a larger minimum time gap and this will be further investigated in the next section on traffic hysteresis.

The experiments on the handling course show instead that shockwaves can be induced and amplified just from the road geometry. Most of the traffic micro-simulation experiments carried out to estimate the impact of ACC and CACC on traffic do not explicitly consider the effect of road slopes or curves. Secondary impacts on traffic, due to instability may be important and new bottleneck locations may appear. In this case, also long time gap platoons have proved to be string-unstable, although first evidence would suggest a stronger dependency from the specific ACC controller logic. For this reason, an attempt to identify the string-stability of the different vehicles was also carried out, although this can only give an indication. A comprehensive analysis would require having the results either of all the possible vehicle combinations in the platoon or the independent tests of each vehicle, which is not the case in the present study.

In Fig. 16 (a) and (b) the average strict string stability indicators in the dynamic platform and handling course are presented, aggregated per vehicle and time gap setting. The vehicle labeling is according to Table 1. In this case, the maximum perturbation magnitude of each vehicle is compared to that of the vehicle directly in front of it. This shows how each vehicle affected the overall stability or instability of the platoon. Results confirm that both time gap and road geometry influence string-stability. For all vehicles, in both experiments, the string-stability indicator takes lower values for larger time gap settings. Concerning the difference between the two experiments, the string stability indicator is consistently higher in the handling course than in the dynamic platform, confirming the negative effect of road geometry on the controller string-stability. Results from individual vehicles seem to suggest that the V8 controller is able to achieve string-stability in all cases, while V4 and V9 seem to be the controllers responsible for the string instability in the handling course experiments with the long time gap setting. As already said, this may well be due to their position in the platoon during the experiments and therefore these results should not be considered as general. It would be interesting to perform more experiments with V8. If confirmed by other tests, it would provide an example of an ACC controller able to improve traffic flow by dampening traffic oscillations.



(a)                                                                              (b)
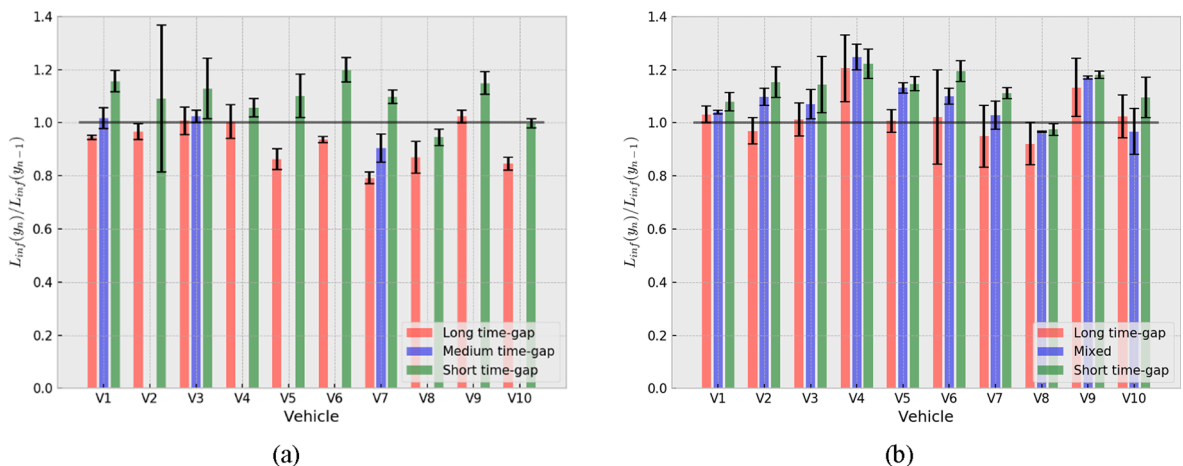
**Fig. 16.** Median strict stability indicator and interquartile range aggregated over the time gap selection and specific vehicle of the platoon in (a) the dynamic platform and (b) the handling course.

### 5.4. Traffic hysteresis

If the string stability analysis, on the one hand, sheds light on the properties of a traffic flow composed by ACC vehicles in terms of shock-wave formation and propagation, on the other hand, it does not say much about the capacity of such a resulting traffic flow. Studying traffic hysteresis adds important elements in this direction.

#### 5.4.1. Dynamic platform

In the dynamic platform experiments, 34 perturbations have been traced and used to evaluate the magnitude of hysteresis, defined as the difference between the average flow during the deceleration and during the acceleration phase. The average hysteresis magnitude for all 34 cases was a 147 veh/hour drop of flow during the acceleration phase. However, the magnitude of hysteresis depends on factors such as the perturbation magnitude and the time gap setting. The maximum drop observed was 458 veh/hour. Four cases of negative hysteresis, for which the acceleration branch averaged a higher flow than the deceleration branch, have also been observed. However, the range of the magnitude of positive hysteresis measured was from 4 to 25 veh/hour, thus very small and within the uncertainty of the experimental data.

As an example of how the different factors may affect the hysteresis magnitude, Fig. 17 shows the speed-flow diagram of 6 perturbations. In particular, Fig. 17(a) shows three 20 km/h perturbations from a target speed of 40 km/hour. The three different cases refer to different time gap settings. The green line represents the short time gap setting, the blue line the medium time gap setting, and the red line the long one. The continuous lines represent the deceleration phase, while the dashed lines represent the acceleration phase. The figure shows that for medium and long time gap settings, the average platoon speed doesn't drop to 20 km/h, while for the short time gap it drops further. This is relevant to the instability of short time gap platoons that have been already discussed. The magnitude of hysteresis is 407 veh/hour for the short time gap, 106 veh/hour for the medium, and 4 veh/hour for the long time gap setting. The short time gap platoon is the only one that produced a flow comparable to that of a platoon of human drivers during the stable phase, around 2000 veh/hour. However, due to considerable hysteresis, the observed flow during the acceleration phase is comparable to the flow produced by the medium time gap platoon. In practice, the string-instability of the short time gap setting platoon jeopardizes the possibility to achieve higher capacity than that achieved by the medium time gap platoon. This would reinforce the aforementioned suggestion to introduce as a requirement for ACC, a minimum time gap able to preserve string-stability.

Fig. 17 (b) also refers to an experiment with a target speed of 40 km/h. However, the three cases all represent platoons with a short time gap setting. The difference is in the perturbation magnitude, which is 10, 15, and 20 km/hour for the green, blue, and red lines respectively. The hysteresis magnitude, in these cases, is 78, 171, and 349 veh/hour respectively, showing that the magnitude of the perturbation can influence hysteresis significantly.

The 34 perturbations were grouped according to the time gap setting and the perturbation magnitude. The median hysteresis and flow during the acceleration phase are then presented in Fig. 18 (a) and (b), together with the first and third quartile values. For the short time gap settings, the hysteresis magnitude is significantly larger than in the other two cases, and it seems to be increasing with the magnitude of the leader's perturbation. This doesn't seem to be the case for the medium and long time gap experiments. Especially for the long time gap, the dampening of the perturbation while it is traveling upstream seems to be more significant for the larger perturbations and the magnitude of hysteresis seems to be decreasing, to even positive hysteresis for perturbations of 25 km/hour. In terms of flow, for small perturbations, the flow during the acceleration phase is still higher for short time gap platoons. For perturbations of higher amplitude, the medium time gap platoons achieved the higher flow during the acceleration phase. The long time gap platoons, while stable and not affected so much by hysteresis, have been consistently achieving the smallest outflow.
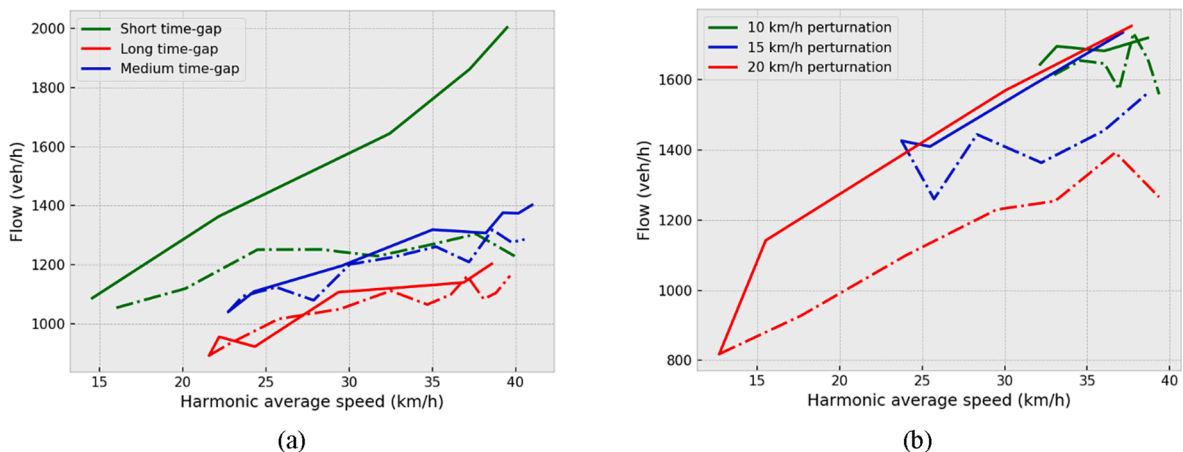


**Fig. 17.** Speed-flow diagrams for platoons with 40 km/h target speed. Chart (a) refers to the case of three platoons with different time gap settings, while chart (b) refers to the case of short time gap platoons subject to three different perturbation magnitudes.
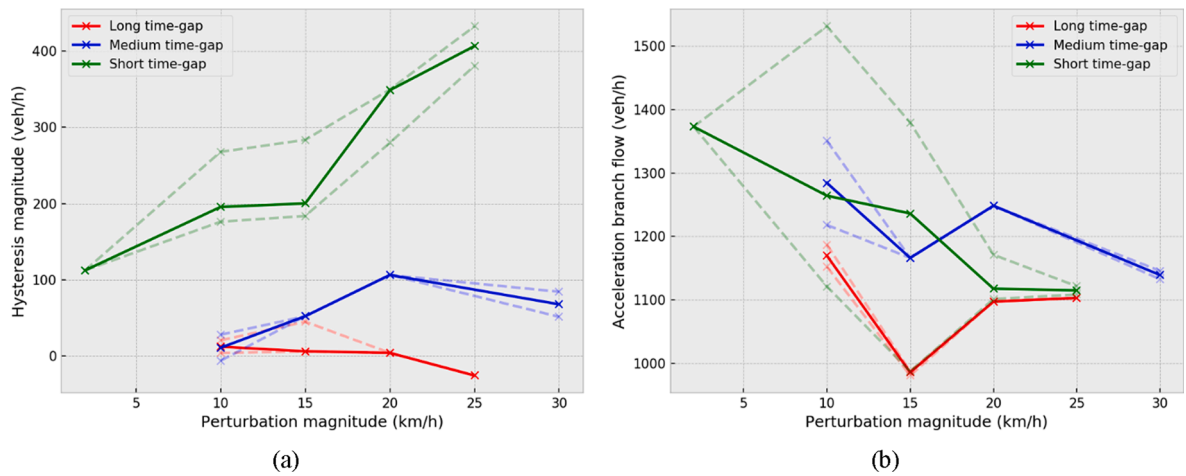
**Fig. 18.** Relationship between the perturbation magnitude and the (a) hysteresis magnitude, (b) flow during the acceleration phase. The median value and the first and third quartiles for 34 experiments in the dynamic platform.
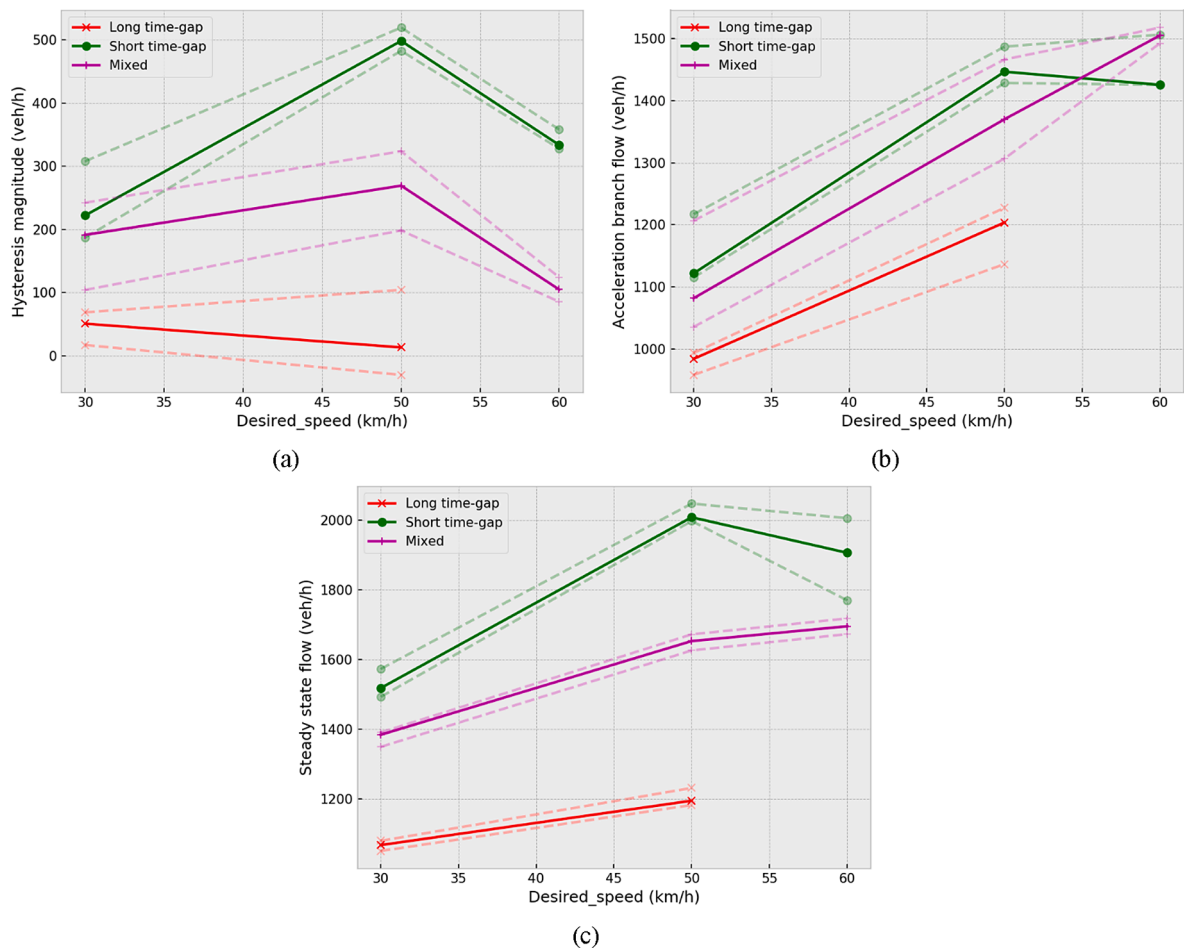


**Fig. 19.** Relationship between the desired speed and (a) the median hysteresis magnitude, (b) the median flow during the acceleration phase (c) the median flow during the steady-state, and the first and third quartiles for 46 experiments in the dynamic platform.

### 5.4.2. Handling course

The oscillations identified in the experiments in the handling course have been 46. There are three different cases of time gap setting: all vehicles keeping the shortest time gap, all vehicles keeping the longest time gap, shortest time gap for all vehicles except one or two vehicles in the middle that used the longest time gap. There is no induced perturbation, and the oscillations are resulting from the road geometry. The average magnitude of hysteresis for all cases is a drop of 215 veh/hour in the flow during the acceleration phase. As in the dynamic platform experiment, there is much variation, this time attributed to the time gap setting and the speed of the leader, which was one of the variables for the experiment. The maximum value observed has been 573 veh/hour and there has been only one case with positive hysteresis of 74 veh/hour.

The perturbations have been grouped according to the desired speed of the leader and the time gap setting. The median hysteresis magnitude and flow during the acceleration phase are presented in Fig. 19 (a) and (b), together with the first and third quartile values. Again, the magnitude of hysteresis is larger for the short time gap platoons. An interesting outcome is that with only one or two vehicles using the longest time gap in the middle of the platoon, the hysteresis was significantly cut down. The long time gap platoons have suffered the least from the hysteresis phenomenon, however, the flow during the acceleration phase is still smaller than the other two cases. The leader's desired speed affects both hysteresis and discharge flow. For the higher speeds, the mixed time gap platoons achieved the highest discharge flow. This result is very sensitive to the specific road geometry of the test track. Hence, it cannot be generalized for different road geometries. However, it is interesting to notice that increasing the time gap of specific vehicles in a platoon can increase the overall traffic efficiency in bottlenecks.
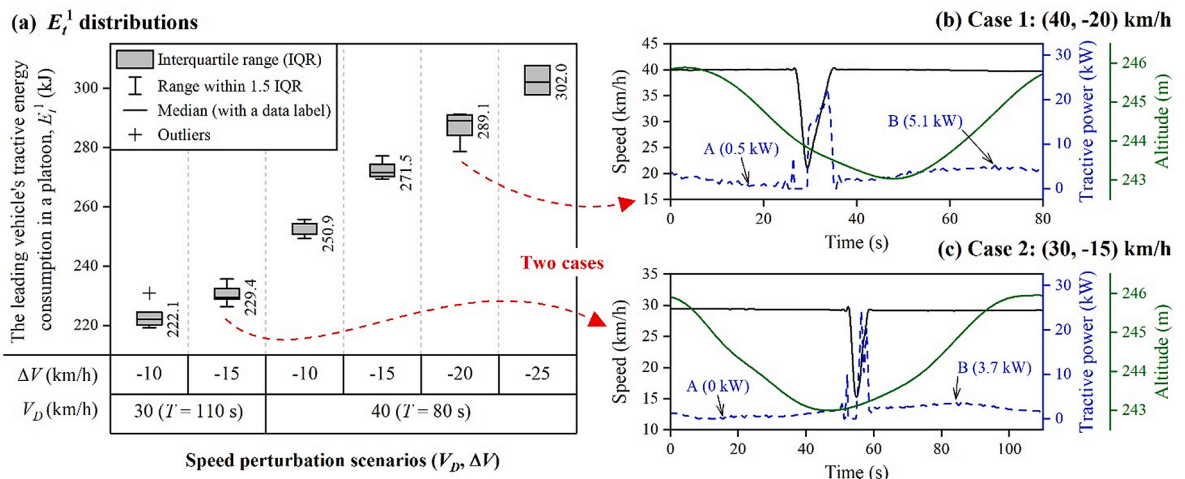
In Fig. 19 (c) the median flow during the steady-state is presented. It is shown that only the shortest time gap setting platoons produced steady-state flow close to that of human drivers, achieving 2000 veh/hour/lane. This result of course is constrained by the available speed range, as the steady-state flow may increase for larger velocity. Moreover, for 60 km/h the variation is increased for the short time gap platoons, decreasing the average flow. This is due to the inability to achieve a true steady-state, which is more prevalent at higher speeds. Again, this is related to the specific geometry and slope of the test site and cannot be generalized. For smoother curves and slopes, the steady state flow could increase with larger platoon speed.

## 5.5. Energy consumption

The desired ACC system targets not only driving safety and traffic stability but also enhanced energy efficiency. This section empirically investigates the energy impacts of current commercial ACC systems in vehicle platoons. The tractive energy consumption ($E_t$, kJ) of vehicles is calculated by using the trajectory data from a set of car-following experiments, which are carried out on both the dynamic platform and the handling course. The findings have revealed several factors (such as the time gap setting, the desired speed, the magnitude of the speed perturbation, and the road slope) that are responsible for energy differences in the ACC platooning.

### 5.5.1. Dynamic platform

The leading vehicle's speed perturbations may be attenuated or amplified when propagating upstream in the platoon, leading to intra-platoon energy differences between the leader and its followers. On the dynamic platform, different speed perturbations are performed by the leading vehicle to uncover their energy impacts on the upstream followers in the platoon.



Fig. 20. Energy and power results of the leading vehicle in platoons tested on the dynamic platform: (a) Distributions of tractive energy consumption ($E_t^1$) in six different speed perturbation scenarios ($V_D$, $\Delta V$); and (b) and (c) speed, tractive power, and altitude profiles of the leading vehicle in two cases of (40, −20) km/h and (30, −15) km/h, respectively.

Fig. 20 (a) shows distributions of the leading vehicle's tractive energy consumption ($E_t^1$) in six different speed perturbation scenarios ($V_D$, $\Delta V$), in which $V_D$ is the desired speed (km/h) and $\Delta V$ is the magnitude of the speed perturbation (km/h). In tick labels of this box plot, $T$ denotes the duration (s) of the trip for tractive energy computation, which is set as 110 s and 80 s for scenarios with the desired speed ($V_D$) of 30 km/h and 40 km/h, respectively. The reason for these settings is that the trips can approximately cover the complete circular test track with a diameter of 300 m and therefore to minimize the energy impacts of the varying road slope.

In this graph, the box indicates the interquartile range (IQR), which is derived from 3 to 7 independent repetitions of platoon tests and can capture the uncertainty surrounding these experiments. Whiskers extend to 1.5 times IQR. The band inside the box is the median (with a data label next to the box). While crosses beyond the whiskers represent outliers. The data suggests that the median estimated $E_t^1$ is 222.1 kJ (IQR = 4.2 kJ) in the scenario of ($V_D$, $\Delta V$) = (30, $-10$) km/h and 229.4 kJ (IQR = 3.6 kJ) in (30, $-15$) km/h. For the other 4 scenarios with the desired speed of $V_D$ = 40 km/h, when increasing the magnitude of the speed perturbation ($\Delta V$) from $-10$ km/h to $-25$ km/h, every $-5$ km/h increment in $\Delta V$ leads to an increase of ~17.0 kJ in the median estimated $E_t^1$; while the corresponding IQR values lie between 3.5 kJ and 10.0 kJ. Generally, IQR values of $E_t^1$ distributions in different scenarios remain small, indicating satisfactorily representativeness of the results. The median estimated $E_t^1$ is found to increase with an increased magnitude of speed perturbation ($\Delta V$).

Fig. 20 (b) and (c) provide speed, tractive power, and altitude profiles of the leading vehicle in two cases of (40, $-20$) km/h and (30, $-15$) km/h, respectively. In both cases, the tractive power reaches a peak (~23.5 kW) at the vehicle acceleration phase. In addition, point A (B) annotated in blue is the minimum (maximum) tractive power during steady-speed driving downslope (upslope). These two points exhibit that the varying road slope of the dynamic platform can lead to tractive power differences no greater than 4.6 kW and 3.7 kW in Case 1 and Case 2, respectively. In both subplots, small positive spikes in tractive power are observed at the onset of braking. They are caused by a temporary and small speed oscillation between the constant-speed and deceleration phases. A plausible explanation for this phenomenon is that varying road slope introduces disturbances during the transition between two phases. Although magnitudes of these speed oscillations are limited, the corresponding acceleration can change moderately, and therefore, according to Equation (7), lead to obvious and high-frequent oscillations of tractive power. Since negative components are not considered, these tractive power oscillations are shown as small positive spikes.

Fig. 21 (a)-(f) display following vehicles' intra-platoon tractive energy increase ($\delta E_{F/L}^i$, %) relative to the leading one in six different speed perturbation scenarios ($V_D$, $\Delta V$), respectively. Different platoons (L-ACC, M$-$ACC, and S-ACC) are color-coded and marked with different symbols (see legend). The marked lines with standard-deviation error bars denote an average of at least two technical replicates. The results demonstrate that S-ACC platoons in six speed perturbation scenarios show a rapid and continuing growth in $\delta E_{F/L}^i$ along the upstream direction. In Scenario 1 and 2 that have the same desired speed ($V_D$) of 30 km/h, S-ACC platoons reach similar peak values of $\delta E_{F/L}^i$ (39.1 % and 35.1 %, respectively) at the last vehicle ($i$ = 6). In Scenario 3–6 with the same $V_D$ of 40 km/h, S-ACC
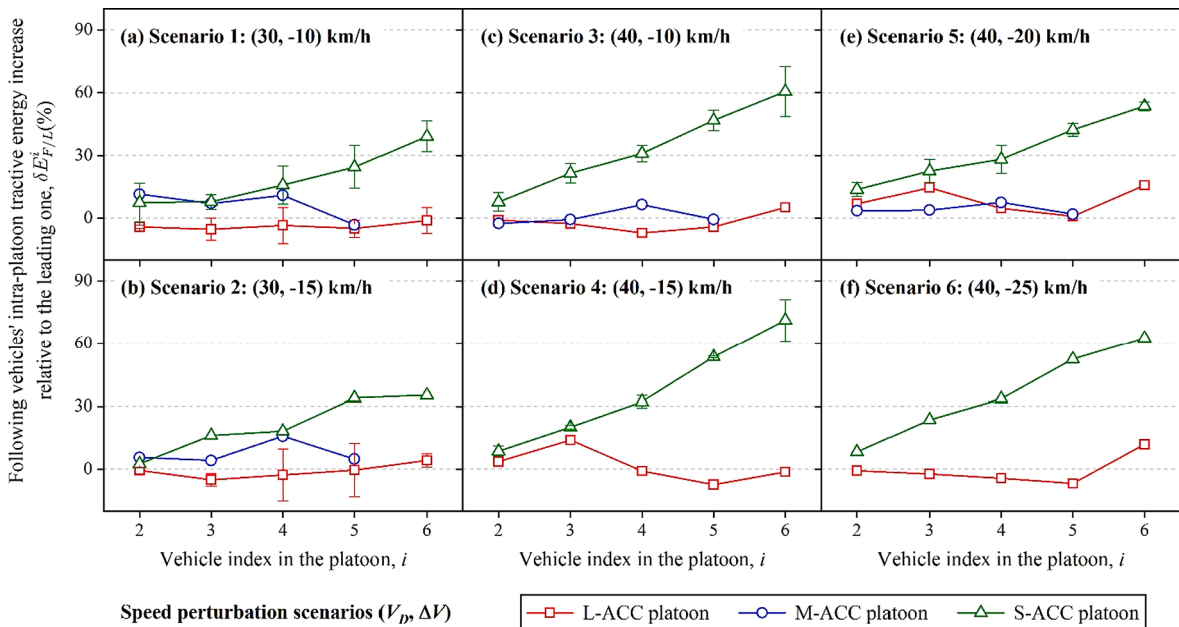


**Fig. 21.** Following vehicles' intra-platoon tractive energy increase ($\delta E_{F/L}^i$, %) in six different speed perturbation scenarios ($V_D$, $\Delta V$) on the dynamic platform: (a) Scenario 1, (30, $-10$) km/h; (b) Scenario 2, (30, $-15$) km/h; (c) Scenario 3, (40, $-10$) km/h; (d) Scenario 4, (40, $-15$) km/h; (e) Scenario 5, (40, $-20$) km/h; and (f) Scenario 6, (40, $-25$) km/h.

platoons reach even higher peak values of $\delta E_{F/L}^i$, ranging from 53.6 % to 71.1 %. On the other hand, both L-ACC and M−ACC platoons in each subplot show no clear trend in $\delta E_{F/L}^i$ values along the upstream direction. These findings provide strong evidence that the leading vehicle's speed perturbations are amplified when propagating upstream in S-ACC platoons, but remain constant or even attenuated in M−ACC or L-ACC platoons. Therefore, ACC platoons with different time gap configurations have different responses to the leading vehicle's speed perturbations.

Instead of individually assessing each follower's energy increase as shown in Fig. 21, Table 4 summarizes the average intra-platoon tractive energy increase ($\Delta\overline{E}_{F/L}$, %) of five following vehicles to evaluate energy impacts of speed perturbations on the whole platoon. The results of M−ACC platoons are not included because of insufficient data. The findings in this table suggest that $\Delta\overline{E}_{F/L}$ values of L-ACC platoons lie between −3.8 % to 8.5 %, indicating small differences in tractive energy between the leading vehicle and its followers in the platoon. S-ACC platoons, on the contrary, result in much larger $\Delta\overline{E}_{F/L}$ values, in which the desired speed ($V_D$) had the most pronounced effect. Specifically, S-ACC platoons have $\Delta\overline{E}_{F/L}$ values between 32.1 % and 37.1 % in scenarios of $V_D = 40$ km/h, nearly doubling those of S-ACC platoons in scenarios of $V_D = 30$ km/h.

### 5.5.2. Handling course

On the handling course with varying road curvature and slope, different platoons perform constant-speed cruising tests to evaluate the overall energy performance of platoons under external disturbances.

Fig. 22 (a)-(c) demonstrate the following vehicles' intra-platoon tractive energy increase ($\delta E_{F/L}^i$) relative to the leading one. Four different platoons (HD, L-ACC, S-ACC, and SL-ACC) are compared in three cruising scenarios on the handling course. Although standard deviation error bars for the four platoons easily overlap, both S-ACC and SL-ACC platoons exhibit an increasing trend in $\delta E_{F/L}^i$ along the upstream direction in each plot, but the former increases more rapidly.

Table 5 summarizes the average intra-platoon tractive energy increase ($\Delta\overline{E}_{F/L}$) of five following vehicles in platoons tested on the handling course. The data suggest that the HD platoon, human drivers of which were instructed to follow their typical driving pattern (to be neither aggressive nor passive), leads to $\Delta\overline{E}_{F/L}$ values ranging from 10.8 % to 16.7 %. The L-ACC platoon results in lower $\Delta\overline{E}_{F/L}$ values of 9.6 % and 2.4% in scenarios of $V_D = 30$ km/h and $V_D = 60$ km/h, respectively. In each scenario, however, the S-ACC platoon leads to the largest $\Delta\overline{E}_{F/L}$ value lying between 24.0 % and 28.9 %. As for the SL-ACC platoon, its $\Delta\overline{E}_{F/L}$ values are between 19.4 % and 21.5 %, much smaller than their S-ACC platoon counterparts.

### 5.5.2.1. Energy analysis of mixed time gap ACC platoons.

To examine energy impacts of long time gap ACC vehicles on SL-ACC (short/long time gap mixed) platoons, Fig. 23. presents four cases for comparing the tractive energy consumption ($E_t$) between the SL-ACC and S-ACC platoons in cruising scenarios of $V_D = 30$ km/h and $V_D = 60$ km/h on the handling course. In each subplot, the SL-ACC and S-ACC platoons have the same vehicle order. The changing indexes, namely, vehicle indexes where the SL-ACC and S-ACC platoons adopt different ACC time gap settings, are indicated by a green rectangle. The vehicle indexes smaller (or larger) than the changing indexes are denoted as downstream (or upstream) indexes. Moreover, the inter-platoon tractive energy difference ($\delta E_{SL/S}^i$, %), between two corresponding vehicles in the SL-ACC and S-ACC platoons, is represented by blue bars above the marked lines.

The results in four cases suggest that, at downstream indexes, the $\delta E_{SL/S}^i$ values are between −0.9 % and 4.6 %, implying negligible energy differences between corresponding vehicles in the SL-ACC and S-ACC platoons. At changing indexes, however, the $\delta E_{SL/S}^i$ values lie between −4.2 % and −18.4 %, indicating that long time gap ACC vehicles in SL-ACC platoons are more energy-efficient than their counterparts in S-ACC platoons. The reason for this is that long time gap ACC vehicles can attenuate speed perturbations propagating from the platoon leader. Benefiting from this, vehicles at upstream indexes in SL-ACC platoons exhibit significant energy savings as well, the values of which ranges from −8.0 % and −22.5 %.

Table 6. compares the total tractive energy consumption between the SL-ACC and S-ACC platoons in the four cases shown in Fig. 23. The $\Delta E_{SL/S}$ values, between −6.1 % and −9.8 %, represent the overall energy savings of SL-ACC platoons relative to their S-ACC counterparts. These results provide definitive evidence that long time gap ACC vehicles can contribute considerably to the platoon energy efficiency.

### 5.6. Safety implications

The same perturbations that have been isolated for the hysteresis analysis are also used to analyze the safety impact of ACC

**Table 4**

Following vehicles' average intra-platoon tractive energy increase ($\Delta\overline{E}_{F/L}$, %) in six speed perturbation scenarios.

| $V_D$(km/h) | 30 | | 40 | | | |
|---|---|---|---|---|---|---|
| $\Delta V$(km/h) | −10 | −15 | −10 | −15 | −20 | −25 |
| L-ACC platoon | −3.8 | −0.9 | −1.9 | 1.6 | 8.5 | −0.4 |
| S-ACC platoon | 18.9 | 21.2 | 33.5 | 37.1 | 32.1 | 36.1 |

*Note*: $V_D$ = desired speed; $\Delta V$ = magnitude of the speed perturbation; L/S-ACC = long, medium, or short time gap adaptive cruise control.
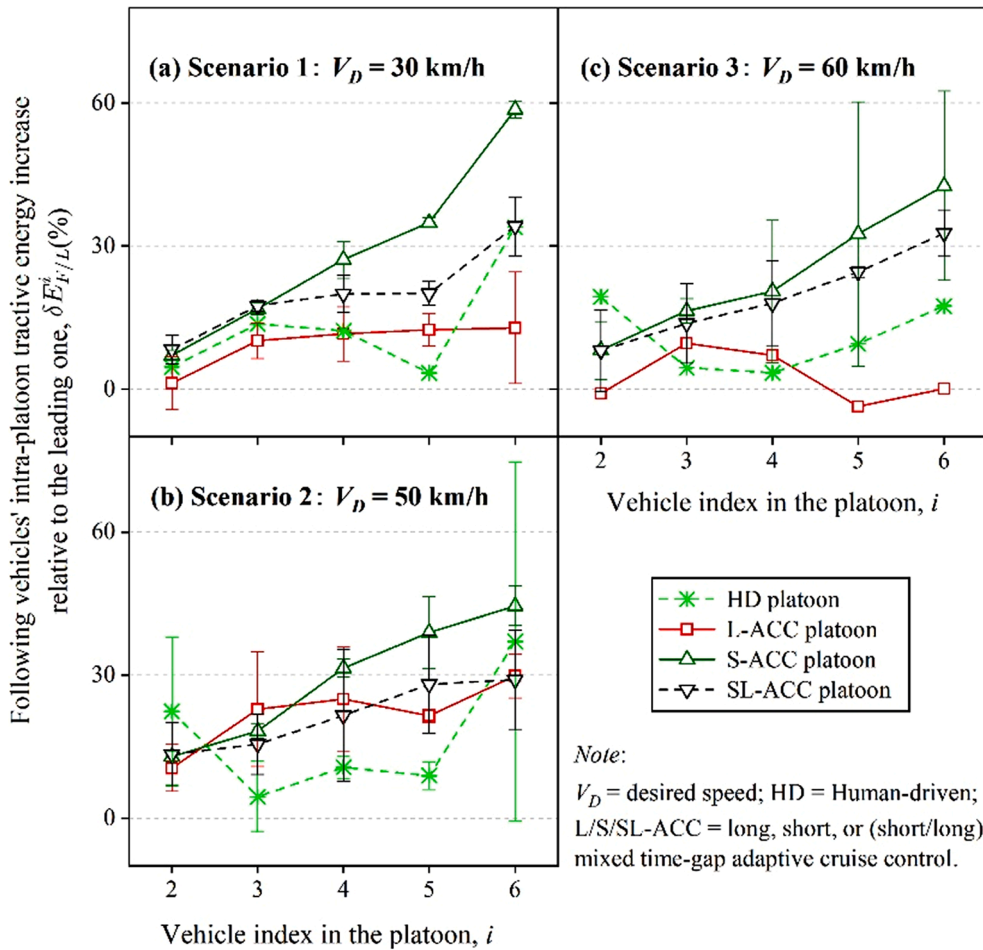
**Fig. 22.** Following vehicles' intra-platoon tractive energy increase ($\delta E_{F/L}^i$, %) in three cruising scenarios on the handling course: (a) Scenario 1, $V_D$ = 30 km/h; (b) Scenario 2, $V_D$ = 50 km/h; and (c) Scenario 3, $V_D$ = 60 km/h.
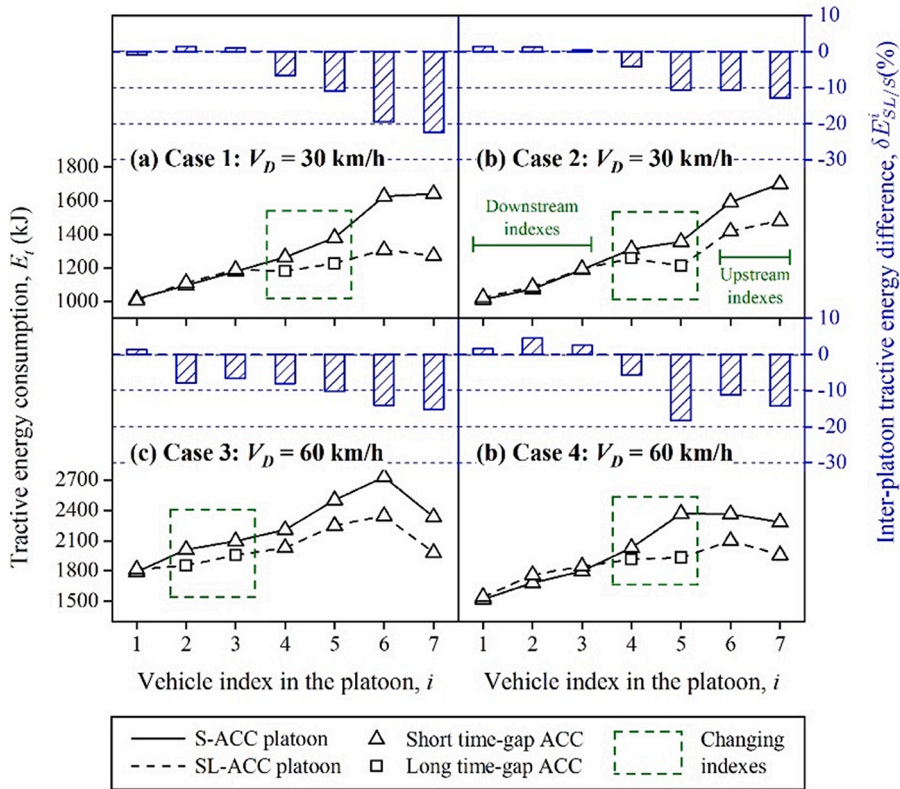
**Table 5**
Following vehicles' average intra-platoon tractive energy increase ($\Delta \overline{E}_{F/L}$, %, relative to that of the platoon leader) in three cruising scenarios.

| $V_D$(km/h) | 30 | 50 | 60 |
|---|---|---|---|
| HD platoon | 13.6 | 16.7 | 10.8 |
| L-ACC platoon | 9.6 | 21.9 | 2.4 |
| S-ACC platoon | 28.9 | 29.2 | 24.0 |
| SL-ACC platoon | 20.0 | 21.5 | 19.4 |

*Note*: $V_D$ = desired speed; HD = Human-driven; L/S/SL-ACC = long, short, or (short/long) mixed time gap adaptive cruise control.

vehicles. In each experiment and for each vehicle, the TTC has been calculated. In Fig. 24 we present the cumulative distributions of the TTC during the perturbations for the experiments in the dynamic platform using the short time gap (a) and the long time gap (b), and for the experiments in the handling course using the short time gap (c) and the long time gap (d), for each vehicle. The distributions only consider the cases with TTC values lower than 100 and the plots focus on the part of the distribution that is related to the smallest TTC values (lower than 7 which account for a maximum probability of 10% in the four charts).

The color of the lines indicates the position of the vehicle in the platoon, with the reddish lines indicating the last vehicles and the greenish lines indicating the first ones. The figure confirms that vehicles with the shortest time gap setting experienced lower safety than those with the longest time gap. In the handling course experiments, even in the case of small perturbations in the leader's speed generated by the road geometry the last vehicles in the platoon experienced a significant number of cases with TTC lower than 4 (and also some cases with TTC lower than 1.5 which is a very strict safety threshold used for TTC), thus highlighting the potential safety threats that platoons of ACC vehicles may trigger in the real world.

**Fig. 23.** The comparison of tractive energy consumption between S-ACC and SL-ACC platoons tested on the handling course. Charts (a) and (b) refer to Case 1 and 2 in the cruising scenario of $V_D = 30$ km/h; charts (c) and (d) refer to Case 3 and 4 in the cruising scenario of $V_D = 60$ km/h.

**Table 6**
Comparison of total tractive energy between SL-ACC and S-ACC platoons on the handling course.

|  | $V_D = 30$ km/h | | $V_D = 60$ km/h | |
| --- | --- | --- | --- | --- |
|  | Case 1 | Case 2 | Case 3 | Case 4 |
| S-ACC platoon (MJ) | 9.2 | 9.2 | 15.7 | 14.0 |
| SL-ACC platoon (MJ) | 8.3 | 8.7 | 14.2 | 13.1 |
| $\Delta E_{SL/S}$(%) | −9.8 | −6.1 | −9.2 | −7.1 |

*Note*: $V_D$ = desired speed; $\Delta E_{SL/S}$ = total inter-platoon tractive energy difference.

Linked to the string stability results, safety deteriorates moving backward in the platoon for the experiment with the short time gap, while it improves for the experiments on the dynamic platform with the long time gap.

It is worth mentioning here that the last vehicles in the platoon experienced safety–critical situations even with fairly mild decelerations imposed by the leading vehicles. In case that stronger perturbations would have been applied, the authors, who were inside the vehicles during the tests, are not confident that crashes could be avoided, even by the expert drivers.

## 6. Discussion and policy implications

Results achieved in the present study have important policy implications. In spite of the introduction of new and more advanced technologies, in the years to come ACC technology is indeed expected to further widespread within the fleet of existing vehicles, and thus to represent the main source of driving automation on motorways for some time ahead. As their number increases, the probability that platoons of ACC driven vehicles form on motorways will also increase, and thus, the appearance of the dynamics identified in the present paper. If left unregulated, the effect of their string unstable behavior will indeed start to emerge, along with a reduction in roads' nominal capacity, increase in vehicles' energy consumption, and possible additional safety risks to drivers. As proposed in the literature, the cooperation between ACC systems enabled by vehicle connectivity can certainly help to address the aforementioned problems, but, in most countries around the world, vehicles' connectivity suffers from regulatory uncertainty, especially for what
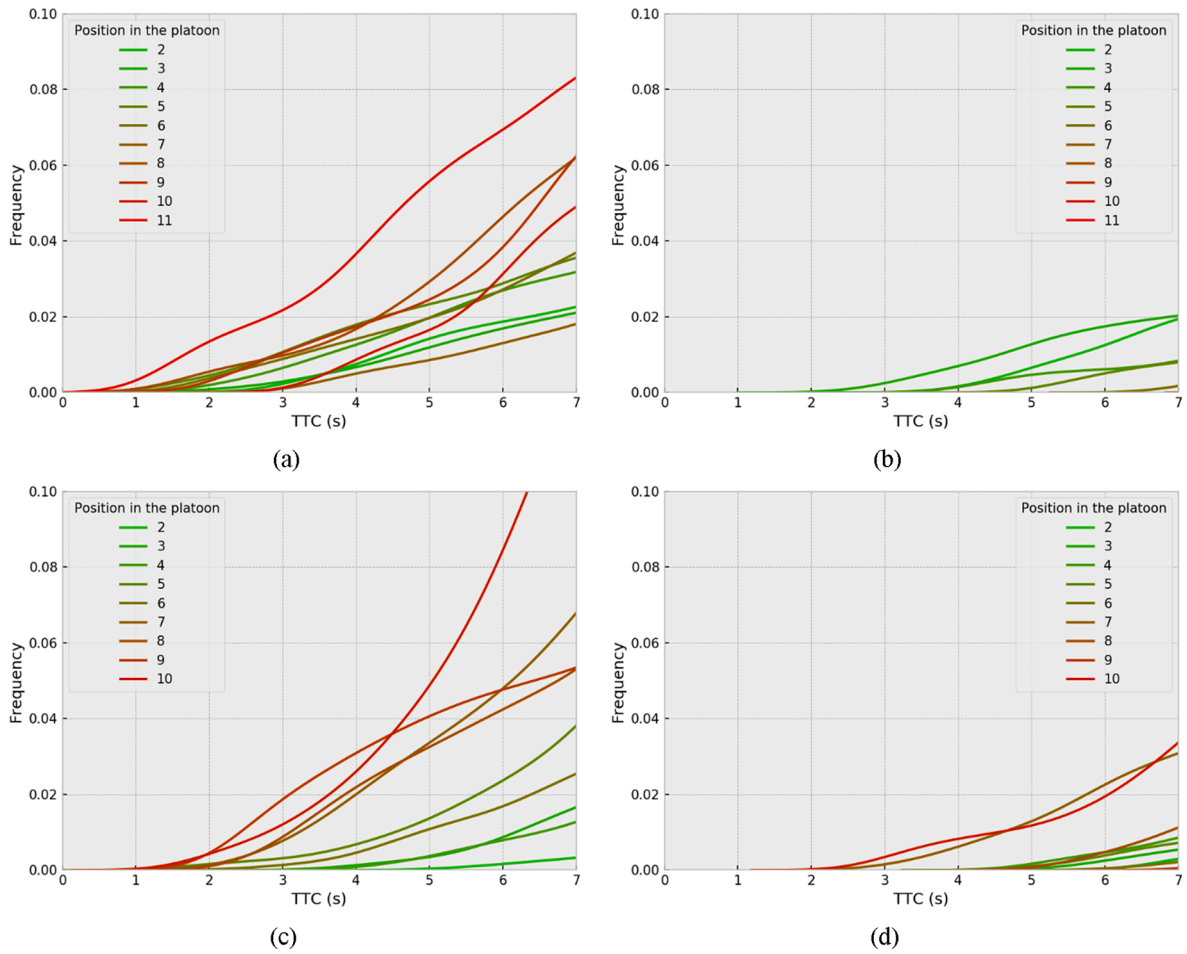
**Fig. 24.** Cumulative distribution of TTC values during perturbations. Charts (a) and (b) refer to the experiments in the dynamic platform while charts (c) and (d) refer to the experiments in the handling course. Charts (a) and (c) refer to experiments with vehicles adopting a short time gap for their ACC, while charts (b) and (d) to long time gap.

concerns the use that vehicles can make of it to cooperate.

A possible solution to mitigate this problem is to introduce string stability in the functional requirements of these systems. At that point, vehicle manufacturers will have different strategies to fulfill this requirement, for example, the increase in the minimum time gap (results from the dynamic platform experiments suggest the existence of a critical time gap able to guarantee both string stability and an acceptable traffic flow), the reduction in the system's response time or the adoption of multi-anticipative behaviors with the system responding not just to the actions of the vehicle immediately in front but also to that of several vehicles ahead (which is also the strategy naturally adopted by attentive human drivers within dense traffic flow). Introducing such functional requirements is not a simple process both because ACC, being considered a comfort system operating under the responsibility of the human driver, escapes international regulation related to vehicle safety and for the intrinsic difficulty to verifying its fulfillment in all possible driving conditions. Further research on this latter aspect is certainly necessary. Unfortunately, this is the only way to avoid that motorway traffic conditions will worsen in the years to come before the introduction of more advanced technologies.

On this latter point, however, additional considerations must be made. In 2020, the first UN regulation on the provisions concerning the approval of automated vehicles had been adopted (UNECE, 2020b). The system considered by the regulation is the Automated Lane Keeping System (ALKS) able to operate without the intervention of the driver on motorways up to a speed of 60 km/h and without changing lane. The regulation refers to the need to respect traffic rules and defines requirements for vehicle safety and the tests to verify that the vehicle fulfills them. The regulation makes no reference to requirements and tests related to vehicles' string stability. However, it defines a minimum time gap that the vehicle will have to respect for different operating speeds. The minimum time gap proposed is however not significantly different from what was observed in the vehicles tested in the present paper (reported in Annex 3). For this reason, there is no guarantee that the first AVs will achieve string stability and address the problems highlighted here. Additional regulations for the approval of more advanced automated driving systems are currently being discussed under the UNECE Working Party on Automated/Autonomous and Connected Vehicles (GRVA). It is interesting to notice that the informal working group focusing on the functional requirements of automated and autonomous vehicles (FRAV) includes among the conceptual

requirements, the need to ensure that automated driving systems will not disrupt the normal flow of traffic (UNECE, 2020c). The translation of this in practical provisions will be the subject of future discussions and the present paper aims at suggesting the introduction of explicit requirements related to the string stability of future automated and autonomous systems. If this will not be achieved, there will be a significant risk that, as in the case of ACC, also for AVs, the promises for higher capacity and stable and smooth traffic flow will be broken.

## 7. Conclusions

The present paper reports the results of a comprehensive test campaign involving 10 market vehicles equipped with ACC. The test campaign has been carried out in two different test-tracks of the ZalaZONE proving ground in Hungary. The tests have been executed at low-speeds (30–60 km/h) with the objective to simulate the behavior of traffic jam assistant systems. The vehicles involved in the experiments had various types of powertrains (internal combustion engine, hybrid electric, and full electric) and were tested with different time gap settings of the ACC systems. The vehicle orders have also been changed to test the effect of different possible experimental variations.

Test results have been analyzed to derive information about the properties of the various ACC systems, to study their string stability, to study the effect of ACC on traffic flow, and to draw inference about the possible implications on energy consumption and vehicle/traffic safety.

In general, results confirm the previous findings in terms of string instability of the ACC. However, they also show that this is strictly dependent on the ACC time gap settings used in the vehicle. Indeed, with a long time gap, vehicles have shown in several experiments a string stable behavior with the magnitude of the perturbation absorbed by the platoon. This has not been a consistent result throughout the whole test campaign and in particular, this was not the case for the experiments in the Handling Course in which the vehicles only showed to be more string stable than with a shorter time gap. This variable behavior suggests that the string instability is not an intrinsic feature of the ACC systems, but it depends on the algorithmic implementation by the vehicle manufacturer. Therefore, the introduction of technical regulations or standards to mandate string stability in the ACC design would contribute towards addressing some of the downsides mentioned in this work. This is particularly important because we have observed that in the presence of string unstable behavior, the ACC also activates hysteresis in the traffic flow, while as soon as the string instability is reduced, the magnitude of the hysteresis is reduced accordingly.

For what concerns energy consumption and safety, results have shown that string unstable behavior has a negative effect on both dimensions. This is certainly another reason to mandate string stability in ACC operations. Indeed, as the number of ACC vehicles on the road increases, the likelihood of having ACC platoons also increases and as such, also the potential risks for drivers and transport networks.

Beyond ACC vehicles, to avoid that in the future similar findings may also concern AVs, string stability should be introduced as a requirement for future automated and autonomous vehicles. This is especially important in the case where the vehicles' cooperation potentially enabled by connectivity will not materialize. Since international regulation on the approval of these technologies is currently being discussed, we believe that this paper may provide important elements to proceed in this direction.

Finally, the paper has shown that road geometry may play a very important role in activating traffic disturbances, especially in the case of string unstable vehicles. Even tests at low speeds have shown that slope (and curvature) variations may induce strong perturbations in the vehicle platoon leading to also considerable safety risks. String unstable vehicles indeed amplify the small variations in the vehicles' speed caused by the delay of the actuator to react to the slope variation. As the length of the platoon increases, also the magnitude of this perturbation increases. In addition, results suggest that road slope may have a reinforcement effect on string instability as the magnitude of the amplification has always been higher in the test track with road slope variation than in the other with almost constant road slope. Among other things, this suggests that traffic models have to progressively embody some elements of the vehicle dynamics that can allow capturing the effect of vehicle technologies and their interaction with the road. Further studies on this aspect will follow.

## CRediT authorship contribution statement

**Biagio Ciuffo:** Conceptualization, Funding Acquisition, Project Administration, Methodology, Supervision, Validation, Writing - original draft, Writing - review & editing. **Konstantinos Mattas:** Methodology, Data Curation, Formal Analysis, Visualization, Validation, Writing - original draft, Writing - review & editing. **Michail Makridis:** Conceptualization, Methodology, Data Curation, Formal Analysis, Visualization, Validation, Writing - original draft, Writing - review & editing. **Giovanni Albano:** Data Curation, Visualization, Writing - original draft. **Aikaterini Anesiadou:** Data Curation, Formal Analysis, Visualization, Validation, Writing - original draft. **Yinglong He:** Methodology, Data Curation, Formal Analysis, Visualization, Validation, Writing - original draft, Writing - review & editing. **Szilard Josvai:** Data Curation, Visualizatio. **Dimitris Komnos:** . **Marton Pataki:** Data Curation, Formal Analysis, Writing - original draft. **Sandor Vass:** Data Curation, Visualization, Validation, Writing - original draft. **Zsolt Szalay:** Conceptualization, Methodology, Supervision, Validation, Writing - original draft, Writing - review & editing.

## Declaration of Competing Interest

The authors declare that they have no known competing financial interests or personal relationships that could have appeared to influence the work reported in this paper.

## Acknowledgments

The views expressed in the paper are purely those of the authors and may not, under any circumstances, be regarded as an official position of the European Commission. The authors are grateful to the technical staff of the ZalaZONE proving ground for supporting the whole campaign, to Inventure Automotive for providing the vehicle-specific CAN bus measuring systems and to Georgios Fontaras from the JRC, to Vincenzo Punzo and Marcello Montanino from the University of Napoli Federico II, to Ludovic Leclerq from the Gustav Eiffel University, to Meng Wang from the Delft Technical University, to Eddie Wilson from the University of Bristol, and to Costantinos Antoniou from the Technical University of Munich for the insightful discussions about the string stability of ACC systems. The authors are also grateful to Ewelina Sujka from the JRC and to Eszter Kaszás from the ZalaZONE proving ground for the administrative support in the organization of the test campaign. Finally, the authors are mostly grateful to the four anonymous reviewers for their very precious comments, which have helped to considerably improve the quality of the manuscript. The experimental campaign described in the paper has been partly funded by the Enlargement and Integration Program of the JRC.

## Appendix A. Supplementary material

Supplementary data to this article can be found online at https://doi.org/10.1016/j.trc.2021.103305.

## References

Ahn, S., Vadlamani, S., Laval, J., 2013. A Method to Account for Non-Steady State Conditions in Measuring Traffic Hysteresis. Transp. Res. Part C: Emerging . Technol. 34, 138–147. https://doi.org/10.1016/j.trc.2011.05.020.

Alonso Raposo, M. (Ed.), Ciuffo, B. (Ed.), Alves Dies, P., Ardente, F., Aurambout, J-P., Baldini, G., Baranzelli, C., Blagoeva, D., Bobba, S., Braun, R., Cassio, L., Chawdhry, P., Christidis, P., Christodoulou, A., Corrado, S., Duboz, A., Duch Brown, N., Felici, S., Fernández Macías, E., Ferragut, J., Fulli, G., Galassi, M-C., Georgakaki, A., Gkoumas , K., Grosso, M., Gómez Vilchez, J., Hajdu, M., Iglesias, M., Julea, A., Krause, J., Kriston, A., Lavalle, C., Lonza, L., Lucas, A., Makridis, M., Marinopoulos, A., Marmier, A., Marques dos Santos, F., Martens, B., Mattas, K., Mathieux, F., Menzel, G., Minarini, F., Mondello, S., Moretto, P., Mortara, B., Navajas Cawood, E., Paffumi, E., Pasimeni, F., Pavel, C., Pekár, F., Pisoni, E., Raileanu, I-C., Sala, S., Saveyn, B., Scholz, H., Serra, N., Tamba, M., Thiel, C., Trentadue, G., Tecchio, P., Tsakalidis, A., Uihlein, A., van Balen, M., Vandecasteele, I., 2019. The future of road transport - Implications of automated, connected, low-carbon and shared mobility, EUR 29748 EN, Publications Office of the European Union, Luxembourg, ISBN 978-92-76-14318-5, http://dx.doi.10.2760/668964, JRC116644. https://publications.europa.eu/en/publication-detail/-/publication/67a07945-96f3-11e9-9369-01aa75ed71a1/language-en (accessed May 25, 2020).

Ard, T., Guo, L., Dollar, A., Fayazi, A., Goulet, N., Jia, Y., Ayalew, B., Vahidi, A., 2020. Energy and flow effects of optimal automated driving in mixed traffic: Vehicle-in-the-loop experimental results. https://arxiv.org/pdf/2009.07872.pdf.

BBC News, 2020. Tesla Autopilot Crash Driver "Was Playing Video Game.", Feb 26.

Bogya, P., Vass, S., Tihanyi, V., 2019. Longitudinal Control with Fuzzy Systems for an Automated Vehicle. Perner's Contacts XIX(Special Issue 2), 58–65 (8 p).

Chen, D., Ahn, S., Laval, J., Zheng, Z., 2014. On the Periodicity of Traffic Oscillations and Capacity Drop: The Role of Driver Characteristics. Transp. Res. Part B: Methodol. 59, 117–136. https://doi.org/10.1016/j.trb.2013.11.005.

Ciuffo, Biagio, Makridis, Michail, Toledo, Tomer, Fontaras, Georgios, 2018. Capability of current car-following models to reproduce vehicle free-flow acceleration dynamics. IEEE Trans. Intell. Transp. Syst. 19 (11), 3594–3603.

Davis, L.C., 2004a. Multilane Simulations of Traffic Phases. Phys. Rev. E 69 (1), 016108. https://doi.org/10.1103/PhysRevE.69.016108.

Davis, L.C., 2004b. Effect of Adaptive Cruise Control Systems on Traffic Flow. Phys. Rev. E: Stat. Nonlin. Soft Matter Phys. 69 (6 Pt 2), 066110 https://doi.org/10.1103/PhysRevE.69.066110.

Davis, L.C., 2012. Stability of adaptive cruise control systems taking account of vehicle response time and delay. Phys. Lett. A 376 (40-41), 2658–2662.

de Winter, Joost C.F., Happee, Riender, Martens, Marieke H., Stanton, Neville A., 2014. Effects of adaptive cruise control and highly automated driving on workload and situation awareness: A review of the empirical evidence. Transp. Res. part F: Traff Psychol. Behav. 27, 196–217.

Dey, Kakan C., Yan, Li, Wang, Xujie, Wang, Yue, Shen, Haiying, Chowdhury, Mashrur, Yu, Lei, Qiu, Chenxi, Soundararaj, Vivekgautham, 2016. A review of communication, driver characteristics, and controls aspects of cooperative adaptive cruise control (CACC). IEEE Trans. Intell. Transp. Syst. 17 (2), 491–509.

Edie, L.C., 1961. Car-Following and Steady-State Theory for Noncongested Traffic. Oper. Res. 9 (1), 66–76. https://doi.org/10.1287/opre.9.1.66.

Farnam, Arash, Sarlette, Alain, 2019. About string stability of a vehicle chain with unidirectional controller. Eur. J. Control 50, 138–144.

Feng, S., Zhang, Y., Li, S.E., Cao, Z., Liu, H.X., Li, L., 2019. String Stability for Vehicular Platoon Control: Definitions and Analysis Methods. Ann. Rev. Control 47, 81–97. https://doi.org/10.1016/j.arcontrol.2019.03.001.

Ford, 2019. New Demonstration Shows Ford Driving Tech Can Help Reduce Frustrating Phantom Traffic Jams This Summer | Ford of Europe | Ford Media Center. https://media.ford.com/content/fordmedia/feu/en/news/2018/07/18/new-demonstration-shows-ford-driving-tech-can-help-reduce-frustr.html (accessed Jul. 22, 2019).

Ge, Jin I., Avedisov, Sergei S., He, Chaozhe R., Qin, Wubing B., Sadeghpour, Mehdi, Orosz, Gábor, 2018. Experimental validation of connected automated vehicle design among human-driven vehicles. Transp. Res. Part C 91, 335–352.

Goñi-Ros, Bernat, Schakel, Wouter J., Papacharalampous, Alexandros E., Wang, Meng, Knoop, Victor L., Sakata, Ichiro, van Arem, Bart, Hoogendoorn, Serge P., 2019. Using advanced adaptive cruise control systems to reduce congestion at sags: An evaluation based on microscopic traffic simulation. Transp. Res. Part C: Emerging . Technol. 102, 411–426.

Gunter, G., Gloudemans, D., Stern, R.E., McQuade, S., Bhadani, R., Bunting, M., Monache, M.L.D., Lysecky, R., Seibold, B., Sprinkle, J., Piccoli, B., Work, D.B., 2019. Are Commercially Implemented Adaptive Cruise Control Systems String Stable? arXiv:1905.02108 [cs].

Han, Jihun, Sciarretta, Antonio, Ojeda, Luis Leon, De Nunzio, Giovanni, Thibault, Laurent, 2018. Safe- and Eco-Driving Control for Connected and Automated Electric Vehicles Using Analytical State-Constrained Optimal Solution. IEEE Trans. Intell. Veh. 3 (2), 163–172. https://doi.org/10.1109/TIV.2018.2804162.

He, Y., Ciuffo, B., Zhou, Q., Makridis, M., Mattas, K., Li, J., Li, Z., Yan, F., Xu, H., 2019. Adaptive Cruise Control Strategies Implemented on Experimental Vehicles: A Review. In: IFAC-Pap., 9th IFAC Symposium on Advances in Automotive Control AAC 2019 52, pp. 21–27. http://dx.doi.10.1016/j.ifacol.2019.09.004.

He, Yinglong, Makridis, Michail, Fontaras, Georgios, Mattas, Konstantinos, Xu, Hongming, Ciuffo, Biagio, 2020a. The energy impact of adaptive cruise control in real-world highway multiple-car-following scenarios. Eur. Transp. Res. Rev. 12 (1) https://doi.org/10.1186/s12544-020-00406-w. ISSN 1867-0717 (online).

He, Yinglong, Wang, Chongming, Zhou, Quan, Li, Ji, Makridis, Michail, Williams, Huw, Lu, Guoxiang, Xu, Hongming, 2020b. Multiobjective component sizing of a hybrid ethanol-electric vehicle propulsion system. Appl. Energy 266, 114843. https://doi.org/10.1016/j.apenergy.2020.114843.

Ioannou, P.A., Stefanovic, M., 2005. Evaluation of ACC Vehicles in Mixed Traffic: Lane Change Effects and Sensitivity Analysis. IEEE Trans. Intell. Transp. Syst. 6 (1), 79–89. https://doi.org/10.1109/TITS.2005.844226.

Kesting, Arne, Treiber, Martin, Schönhof, Martin, Kranke, Florian, Helbing, Dirk, 2007. Jam-Avoiding Adaptive Cruise Control (ACC) and Its Impact on Traffic Dynamics. In: Schadschneider, Andreas, Pöschel, Thorsten, Kühne, Reinhart, Schreckenberg, Michael, Wolf, Dietrich E. (Eds.), Traffic and Granular Flow'05. Springer Berlin Heidelberg, Berlin, Heidelberg, pp. 633–643. https://doi.org/10.1007/978-3-540-47641-2_62.

Kesting, A., Treiber, M., Schönhof, M., Helbing, D., 2008. Adaptive Cruise Control Design for Active Congestion Avoidance. Transp. Res. Part C: Emerging . Technol. 16 (6), 668–683. https://doi.org/10.1016/j.trc.2007.12.004.

Knoop, Victor L., Wang, Meng, Wilmink, Isabel, Hoedemaeker, D. Marika, Maaskant, Mark, Van der Meer, Evert-Jeen, 2019. Platoon of SAE Level-2 Automated Vehicles on Public Roads: Setup, Traffic Interactions, and Stability. Transp. Res. Rec. 2673 (9), 311–322. https://doi.org/10.1177/0361198119845885.

Laureshyn, A., Svensson, Å., Hydén, C., 2010. Evaluation of Traffic Safety, Based on Micro-Level Behavioural Data: Theoretical Framework and First Implementation. Accid. Anal. Prev. 42 (6), 1637–1646. https://doi.org/10.1016/j.aap.2010.03.021.

Laureshyn, A., Johnsson, C., Ceunynck, T.D., Svensson, \AAse, de Goede, M., Saunier, N., Włodarek, P., van der Horst, R., Daniels, S., 2016. Review of Current Study Methods for VRU Safety. Appendix 6 – Scoping Review: Surrogate Measures of Safety in Site-Based Road Traffic Observations: Deliverable 2.1 – Part 4.

Laval, J.A., 2011. Hysteresis in Traffic Flow Revisited: An Improved Measurement Method. Transp. Res. Part B: Methodol. 45 (2), 385–391. https://doi.org/10.1016/j.trb.2010.07.006.

Laval, J.A., Leclercq, L., 2010. A Mechanism to Describe the Formation and Propagation of Stop-and-Go Waves in Congested Freeway Traffic. Philosoph. Trans. Roy. Soc. A: Math. Phys. Eng. Sci. 368 (1928), 4519–4541. https://doi.org/10.1098/rsta.2010.0138.

Li, Y., Li, Z., Wang, H., Wang, W., Xing, L., 2017. Evaluating the Safety Impact of Adaptive Cruise Control in Traffic Oscillations on Freeways. Accid. Anal. Prev. 104, 137–145. https://doi.org/10.1016/j.aap.2017.04.025.

Li, D., Wagner, P., 2019. Impacts of Gradual Automated Vehicle Penetration on Motorway Operation: A Comprehensive Evaluation. Eur. Transp. Res. Rev. 11 (1), 36. https://doi.org/10.1186/s12544-019-0375-3. 12.

Mahmud, S.M. Sohel, Ferreira, Luis, Hoque, Md. Shamsul, Tavassoli, Ahmad, 2019. Micro-Simulation Modelling for Traffic Safety: A Review and Potential Application to Heterogeneous Traffic Environment. IATSS Res. 43 (1), 27–36. https://doi.org/10.1016/j.iatssr.2018.07.002.

Makridis, Michail, Mattas, Konstantinos, Ciuffo, Biagio, 2020a. Response Time and Time Headway of an Adaptive Cruise Control. An Empirical Characterization and Potential Impacts on Road Capacity. IEEE Trans. Intell. Transp. Syst. 21 (4), 1677–1686.

Makridis, Michail, Mattas, Konstantinos, Ciuffo, Biagio, Re, Fabrizio, Kriston, Akos, Minarini, Fabrizio, Rognelund, Greger, 2020b. Empirical Study on the Properties of Adaptive Cruise Control Systems and Their Impact on Traffic Flow and String Stability. Transp. Res. Rec. 2674 (4), 471–484.

Makridis, M., Leclercq, L., Mattas, K., Ciuffo, B., 2020c. The impact of driving homogeneity due to automation and cooperation of vehicles on uphill freeway sections. Eur. Transp. Res. Rev. 12, 15. https://doi.org/10.1186/s12544-020-00407-9.

Makridis, M., Mattas, K., Anesiadou, A., Ciuffo, B., 2021. OpenACC. An open database of car-following experiments to study the properties of commercial ACC systems. Transp. Res. Part C: Emerging Technologies. 125, in press. doi:10.1016/j.trc.2021.103047.

Manolis, D., Spiliopoulou, A., Vandorou, F., Papageorgiou, M., 2020. Real time adaptive cruise control strategy for motorways. Transp. Res. Part C: Emerging . Technol. 115, 102617.

Marsden, Greg, McDonald, Mike, Brackstone, Mark, 2001. Towards an understanding of adaptive cruise control. Transp. Res. Part C 9 (1), 33–51.

Martinez, J., Canudas-de-Wit, C., 2007. Safe Longitudinal Control for Adaptive Cruise Control and Stop-and-Go Scenarios. IEEE Trans. Intell. Transp. Syst. 15 (2), 246–258.

Mattas, Konstantinos, Makridis, Michalis, Hallac, Pauliana, Raposo, María Alonso, Thiel, Christian, Toledo, Tomer, Ciuffo, Biagio, 2018. Simulating Deployment of Connectivity and Automation on the Antwerp Ring Road. IET Intel. Transport Syst. 12 (9), 1036–1044. https://doi.org/10.1049/itr2.v12.910.1049/iet-its.2018.5287.

Milanés, V., Shladover, S.E., 2014. Modeling Cooperative and Autonomous Adaptive Cruise Control Dynamic Responses Using Experimental Data. Transp. Res. Part C: Emerg. Technol. 48 (Supplement C), 285–300. https://doi.org/10.1016/j.trc.2014.09.001.

Montanino, M., Monteil, J., Punzo, V., 2021. From homogeneous to heterogeneous traffic flows: Lp String stability under uncertain model parameters. Transp. Res. Part B: Methodol. 146, 136–154. https://doi.org/10.1016/j.trb.2021.01.009.

Montanino, M., Punzo, V., 2021. On string stability of a mixed and heterogeneous traffic flow: A unifying modelling framework. Transp. Res. Part B: Methodol. 144, 133–154. https://doi.org/10.1016/j.trb.2020.11.009.

Monteil, J., Bouroche, M., Leith, D.J., 2019. L2 and Linfinity Stability Analysis of Heterogeneous Traffic With Application to Parameter Optimization for the Control of Automated Vehicles. IEEE Trans. Control Syst. Technol. 27 (3), 934–949. https://doi.org/10.1109/TCST.2018.2808909.

Ploeg, Jeroen, Shukla, Dipan P., van de Wouw, Nathan, Nijmeijer, Henk, 2014. Controller Synthesis for String Stability of Vehicle Platoons. IEEE Trans. Intell. Transp. Syst. 15 (2), 854–865.

Punzo, V., Ciuffo, B., Montanino, M., 2012. Can Results of car-following Model Calibration Based on Trajectory Data be Trusted? Transp. Res. Rec. 2315 (1), 11–24. https://doi.org/10.3141/2315-02.

SAE International, 2018. Taxonomy and Definitions for Terms Related to Driving Automation Systems for On-Road Motor Vehicles , J3016_201806.

Saifuzzaman, M., Zheng, Z., Haque, Md.M., Washington, S., 2017. Understanding the Mechanism of Traffic Hysteresis and Traffic Oscillations through the Change in Task Difficulty Level. Transp. Res. Part B: Methodol. 105, 523–538. https://doi.org/10.1016/j.trb.2017.09.023.

Shladover, S.E., Su, D., Lu, X.-Y., 2012. Impacts of Cooperative Adaptive Cruise Control on Freeway Traffic Flow. Transp. Res. Rec. 2324 (1), 63–70. https://doi.org/10.3141/2324-08.

Shladover, S.E., Nowakowski, C., Lu, X.-Y., Ferlis, R., 2015. Cooperative Adaptive Cruise Control: Definitions and Operating Concepts. Transp. Res. Rec. 2489 (1), 145–152. https://doi.org/10.3141/2489-17.

Shladover, S.E., 2018. Connected and Automated Vehicle Systems: Introduction and Overview. J. Intell. Transp. Syst. 22 (3), 190–200. https://doi.org/10.1080/15472450.2017.1336053.

Stern, R.E., Cui, S., Delle Monache, M.L., Bhadani, R., Bunting, M., Churchill, M., Hamilton, N., Pohlmann, H., Wu, F., Piccoli, B., Seibold, B., Sprinkle, J., Work, P.B., 2018. Dissipation of stop-and-go waves via control of autonomous vehicles: Field experiments. Transp. Res. Part C 89, 205–221.

Sun, J., Zheng, Z., Sun, J., 2018. Stability Analysis Methods and Their Applicability to Car-Following Models in Conventional and Connected Environments. Transp. Res. Part B: Methodol. 109, 212–237. https://doi.org/10.1016/j.trb.2018.01.013.

Szalay, Z., Hamar, Z., Nyerges, Á., 2019. Novel design concept for an automotive proving ground supporting multilevel CAV development. Int. J. Vehicle Design 80 (1), 1–22.

Talebpour, Alireza, Mahmassani, Hani S., 2016. Influence of connected and autonomous vehicles on traffic flow stability and throughput'. Transp. Res. C Emerg. Technol. 71, 143–163.

Treiber, M., Helbing, D., 2001. Microsimulations of Freeway Traffic Including Control Measures. at - Automatisierungstechnik Methoden und Anwendungen der Steuerungs-. Regelungs- und Informationstechnik 49 (11/2001), 478. https://doi.org/10.1524/auto.2001.49.11.478.

Tu, Y., Wang, W., Li, Y., Xu, C., Xu, T., Li, X., 2019. Longitudinal Safety Impacts of Cooperative Adaptive Cruise Control Vehicle's Degradation. J. Saf. Res. 69, 177–192. https://doi.org/10.1016/j.jsr.2019.03.002.

UNECE, 2020. Working Party on Automated/Autonomous and Connected Vehicles (GRVA). Available online at https://www.unece.org/trans/main/wp29/meeting_docs_grva.html (accessed May 26, 2020).

UNECE, 2020. Proposal for a new UN Regulation on uniform provisions concerning the approval of vehicles with regards to Automated Lane Keeping System. Available online at http://www.unece.org/trans/themes/transtheme-its/automated-vehicles/achievements.html (accessed June 26, 2020).

UNECE, 2020. Draft Report on Common Functional Performance Requirements for Automated and Autonomous Vehicles. Available online at https://wiki.unece.org/download/attachments/92013888/FRAV-03-05.pdf?api=v2 (accessed June 26, 2020).

Vahidi, A., Eskandarian, A., 2003. Research Advances in Intelligent Collision Avoidance and Adaptive Cruise Control. IEEE Trans. Intell. Transp. Syst. 4 (3), 143–153.

van Arem, B., van Driel, C.J.G., Visser, R., 2006. The Impact of Cooperative Adaptive Cruise Control on Traffic-Flow Characteristics. IEEE Trans. Intell. Transp. Syst. 7 (4), 429–436. https://doi.org/10.1109/TITS.2006.884615.

Wang, M., Hoogendoorn, S.P., Daamen, W., van Arem, B., Shyrokau, B., Happee, R., 2018. Delay-compensating strategy to enhance string stability of adaptive cruise controlled vehicles. Transportmetr. B: Transp. Dyn. 6 (3), 211–229. https://doi.org/10.1080/21680566.2016.1266973.

Wilson, R.E., Ward, J.A., 2011. Car-Following Models: Fifty Years of Linear Stability Analysis – a Mathematical Perspective. Transp. Plan. Technol. 34 (1), 3–18. https://doi.org/10.1080/03081060.2011.530826.

Xiao, Lingyun, Gao, Feng, 2010. A Comprehensive Review of the Development of Adaptive Cruise Control Systems. Veh. Syst. Dyn. 48 (10), 1167–1192. https://doi.org/10.1080/00423110903365910.

Xiao, Lingyun, Gao, Feng, 2011. Practical String Stability of Platoon of Adaptive Cruise Control Vehicles. IEEE Trans. Intell. Transp. Syst. 12 (4), 1184–1194.

Zheng, Z., Ahn, S., Chen, D., Laval, J., 2011. Freeway Traffic Oscillations: Microscopic Analysis of Formations and Propagations Using Wavelet Transform. Transp. Res. Part B: Methodol. 45 (9), 1378–1388. https://doi.org/10.1016/j.trb.2011.05.012.

Zhu, Lei, Gonder, Jeffrey, Bjarkvik, Eric, Pourabdollah, Mitra, Lindenberg, Bjorn, 2019. An Automated Vehicle Fuel Economy Benefits Evaluation Framework Using Real-World Travel and Traffic Data. IEEE Intell. Transp. Syst. Mag. 11 (3), 29–41. https://doi.org/10.1109/MITS.511764510.1109/MITS.2019.2919537.

Zhou, J., Peng, H., 2005. Range Policy of Adaptive Cruise Control Vehicles for Improved Flow Stability and String Stability. IEEE Trans. Intell. Transp. Syst. 6 (2), 229–237.